Coordination Chemistry Reviews, 65 (1985) 167–218
Elsevier Science Publishers B.V., Amsterdam – Printed in The Netherlands

STRUCTURAL AND ELECTRONIC PROPERTIES OF SOME POLYMOLYBDATES REDUCIBLE TO MOLYBDENUM BLUES

R. IAN BUCKLEY and ROBIN J.H. CLARK

Christopher Ingold Laboratories, University College London, 20 Gordon Street, London, WC1H 0AJ (Gt. Britain)

(Received 1 October 1984)

CONTENTS

A. INTRODUCTION

The isopoly- and heteropolyanions of vanadium, niobium, tantalum, molybdenum, and tungsten have received a great deal of attention in the past [1]. Many isopolyanions form coloured heteropolyanions in solution and heteropolymolybdates have been employed as analytical reagents for many years [2]. Structurally they are of considerable interest, and polymolybdates and -tungstates have been extensively investigated [3,4]. The electronic structures of polyanions are fairly well understood but the nature of their reduced analogues, the so called "heteropoly blues" (a generic name derived from their intense colouration) is, however, not yet fully resolved [4]. Classification of the reduced blues as mixed-valence complexes [5] contain-

0010-8545/85/$18.20

ing both Mo^{V} and Mo^{VI} is not entirely clear, the one-electron blues being thought to be localised-valence species whereas the more highly reduced ones may be delocalised-valence species.

Recent reviews of the properties of both polymolybdates and polytungstates have been published. Tytko and Glemser [6] cover the mechanisms of polyanion formation whilst Weakley [3] and Pope [4] discuss structural types and heteropoly blues, respectively.

We have chosen to describe the various structural and electronic properties of the polymolybdates, in particular those of anions which are reducible in one-electron steps to molybdenum blues. We have also restricted the discussion largely to the one-electron blues which, along with many other further reduced molybdates, are mixed-valence in character (unlike heteropoly blues such as $[SiMo_2^{V}W_{10}^{VI}O_{40}]^{6-}$).

B. STRUCTURAL ASPECTS OF SOME POLYMOLYBDATES

(i) Structural types and their reducibility to molybdenum blues

The reducibility of polymolybdates to mixed-valence blues has been rationalised by Pope [7] and Nomiya and Makoto [8]. Electronic and structural comparisons can be made between types of molybdenum–oxygen bonds in three classes of polymolybdate and monomeric molybdenum oxo-complexes.

Polymolybdate structures can be categorised in terms of the number of unshared terminal oxygen atoms bonded to each molybdenum atom. Type a structures can be compared to monomeric $[Mo^{VI}OL_5]^{-}$ ions (where the ion L has a single negative charge) where the molybdenum atom is in an approximately tetragonal site with symmetry close to C_{4v}. The single oxygen atom is obviously unshared. Polyanions with type b structures have two unshared oxygen atoms in a *cis*-configuration. A *cis*-dioxo complex of this sort is analogous with $[Mo^{VI}O_2L_4]^{2-}$ ions. Type c polymolybdates possess both sorts of metal sites and this structure is thought only to be adopted by the degradation products of other species, i.e. $[X^{n+}Mo_{11}O_{39}]^{(12-n)-}$ and $[(X^{n+})_2Mo_{17}O_{61}]^{(20-2n)-}$. These two anions are derived from the partial hydrolysis of $[X^{n+}Mo_{12}O_{40}]^{(8-n)-}$ and $[(X^{n+})_2Mo_{18}O_{62}]^{(16-2n)-}$, respectively [9,10]. The classification of polymolybdates into structural types is shown in Table 1.

The existence of compounds containing the $[Mo^{V}O_2L_4]^{3-}$ ion has not been established. The molybdenum ion has a d^1 valence electron configuration (Mo^{V}) and the non-existence of this type of anion compares with the non-reducibility of the type b polymolybdates. It is the type a and type c polymolybdate structures which are reducible to blues. Type b complexes

TABLE 1

Structural types of isopoly- and heteropolymolybdates and their reducibility to molybdenum blues

Type a. These molybdates are analogous to $[MoOL_5]^-$ complexes. The molybdenum atoms are in approximately tetragonal sites of nearly C_{4v} symmetry with a single unshared terminal oxygen atom. Molybdates with structures of this type are reducible in one-electron steps.

Formula type	Structure name	Central group	Hetero-atoms, X	Symmetry
$[X^{n+}Mo_{12}O_{40}]^{(8-n)-}$	Keggin	XO_4	Si^{IV}, Ge^{IV}, P^V, As^V, V^V,	α-isomer, T_d
(V- or W-substituted ions are also well established)			Ti^{IV}, Zr^{IV}, In^{III}	β-isomer, C_{3v}
$[(X^{n+})_2Mo_{18}O_{62}]^{(16-2n)-}$	Dawson	XO_4	P^V, As^V	A-isomer, D_{3d} [a] B-isomer, D_{3h}
$[M_6O_{19}]^{n-}$ (M = Mo, Mo + W, or Mo + V) [b]	Lindqvist–Aaronsson	–	–	O_h

Type b. These molybdates are analogous to $[MoO_2L_4]$ complexes. The molybdenum atoms have two *cis* oxygen atoms which are unshared. *Cis*-dioxo molybdates are not reducible [c] and complexes of the type $[MoO_2L_4]^{n-}$ are unknown where the molybdenum ion has a d^1 valence electron configuration (i.e. Mo^V).

Formula Type	Central Group	Hetero-atoms, X	Symmetry
$[(X^{n+})_2Mo_5O_{23}]^{(16-2n)-}$	XO_4	P^V	T_d
$[X^{n+}Mo_6O_{24}]^{(12-n)-}$	XO_6	Te^{VI}, I^{VII}	O_h
$[X^{n+}Mo_6O_{24}H_6]^{(6-n)-}$	XO_6	Al^{III}, Cr^{III}, Co^{III}, Fe^{III}, Ga^{III}, Rh^{III}, Mn^{II}, Co^{II}, Ni^{II}, Cu^{II}, Zn^{II}	O_h
$[X^{n+}Mo_9O_{32}]^{(10-n)-}$	XO_6	Mn^{IV}, Ni^{IV}	O_h
$[(X^{n+})_2Mo_{10}O_{38}H_4]^{(12-2n)-}$	XO_6	Co^{III}	O_h
$[X^{n+}Mo_{12}O_{42}]^{(12-n)-}$	XO_6	Ce^{IV}, Th^{IV}, U^{IV}	O_h
$[Mo_7O_{24}]^{6-}$	–	–	C_{2v}
$[Mo_8O_{26}]^{4-}$			

Type c. These molybdates do not have monomeric analogues and the structures contain both mono-oxo and *cis*-dioxo terminal oxygen atoms. They are reducible in one-electron steps.

Formula Type	Structure name	Central group	Hetero-atoms, X	Symmetry
$[X^{n+}Mo_{11}O_{39}]^{(12-n)-}$	related to Keggin	XO_4	See Keggin	C_s
$[(X^{n+})_2Mo_{17}O_{61}]^{(20-2n)-}$	related to Dawson	XO_4	see Dawson	ca. T_d

[a] The two isomers have been called α-(B-isomer) and β-(A-isomer) Dawson structures by Pope [17] to be consistent with the Keggin nomenclature.

[b] Mono-substituted anions and one-electron reduced species have C_{4v} symmetry.

[c] $[Mo_7O_{24}]^{6-}$ and $[Mo_8O_{26}]^{4-}$ (or the ion $[H_2Mo_8O_{28}]^{6-}$) are known to be reduced when irradiated with either ultraviolet light or γ-rays [11].

with *cis*-dioxo groups are not. The addition of a single electron to $[Mo^{VI}OL_5]^-$ ions of C_{4v} symmetry produces the analogue of a one-electron blue and the unpaired electron resides in a b_2 (d_{xy}) orbital (see later).

The heptamolybdate anion $[Mo_7O_{24}]^{6-}$ can be reduced by irradiation with either ultraviolet light [11,12] or γ-rays [13]. This and other anions containing *cis*-dioxo groups only are easily reduced but the reduction mechanism involves an interaction between anion and cation in both the solid state and in solution. A charge-transfer complex is formed during the irradiation and electron transfer occurs via hydrogen bonds between anion and counterion [12].

The isopoly- and heteropolymolybdates with which we are concerned are therefore of the following types (all containing an unshared oxygen atom in a terminal position): Keggin anions [14] of formula $[X^{n+}Mo_{12}O_{40}]^{(8-n)-}$, Lindqvist–Aaronsson anions [15] of formula $[Mo_6O_{19}]^{n-}$ and the Dawson anions [16] of formula $[(X^{n+})_2Mo_{18}O_{62}]^{(16-2n)-}$.

(ii) The structures of reducible polyanions

The Keggin structure for dodecamolybdates, $[X^{n+}Mo_{12}O_{40}]^{(8-n)-}$

The Keggin series of polyanions [14] has the point symmetry T_d of the central XO_4 tetrahedron. The structure consists of groups of three edge-linked MoO_6 octahedra (i.e., Mo_3O_{13} units) with the molybdenum atom defining an equilateral triangle. The molybdenum atoms are displaced from the centres of their respective octahedra through Coulombic repulsions. An almost regular cubo-octahedron is thus formed by the molybdenum atoms with Mo_3O_{13} groups sharing corners. Anions of this type therefore possess both edge- and corner-linked MoO_6 octahedra. The α-isomer, so described, is shown in Fig. 1a, b. A second (β) isomer, energetically less stable than the first [17], can be derived therefrom and is shown in Fig. 1c, d. The β-isomer is obtained by rotating one Mo_3O_{13} group through 60° about a C_3 axis through a face of the central XO_4 tetrahedron. Rotation by 60° of each of the Mo_3O_{13} groups produces five isomers in all [18]. It has generally been assumed [19] that β-12-molybdates are isostructural with β-$[SiW_{12}O_{40}]^{4-}$, and thus that they have C_{3v} symmetry. However, this has only very recently been proven in one instance to be the case, specifically for the $[PMo_{12}O_{40}]^{7-}$ ion in $Ca_{0.5}H_6[PMo_{12}O_{40}] \cdot$ ca. $18H_2O$ [19a]. It is probable that, in addition to the α-isomers, β-isomers exist for $[SiMo_{12}O_{40}]^{4-}$ and $[GeMo_{12}O_{40}]^{4-}$, although possibly not for $[PMo_{12}O_{40}]^{3-}$ or $[AsMo_{12}O_{40}]^{3-}$ [19].

The main differences between α- and β-Keggin anions are as follows. The β-isomers tend to undergo one-electron reduction more readily than do the α-isomers; polarographically, the two isomers are similar but the half-wave reduction potentials are more positive for the β-isomers [19]. The absorption

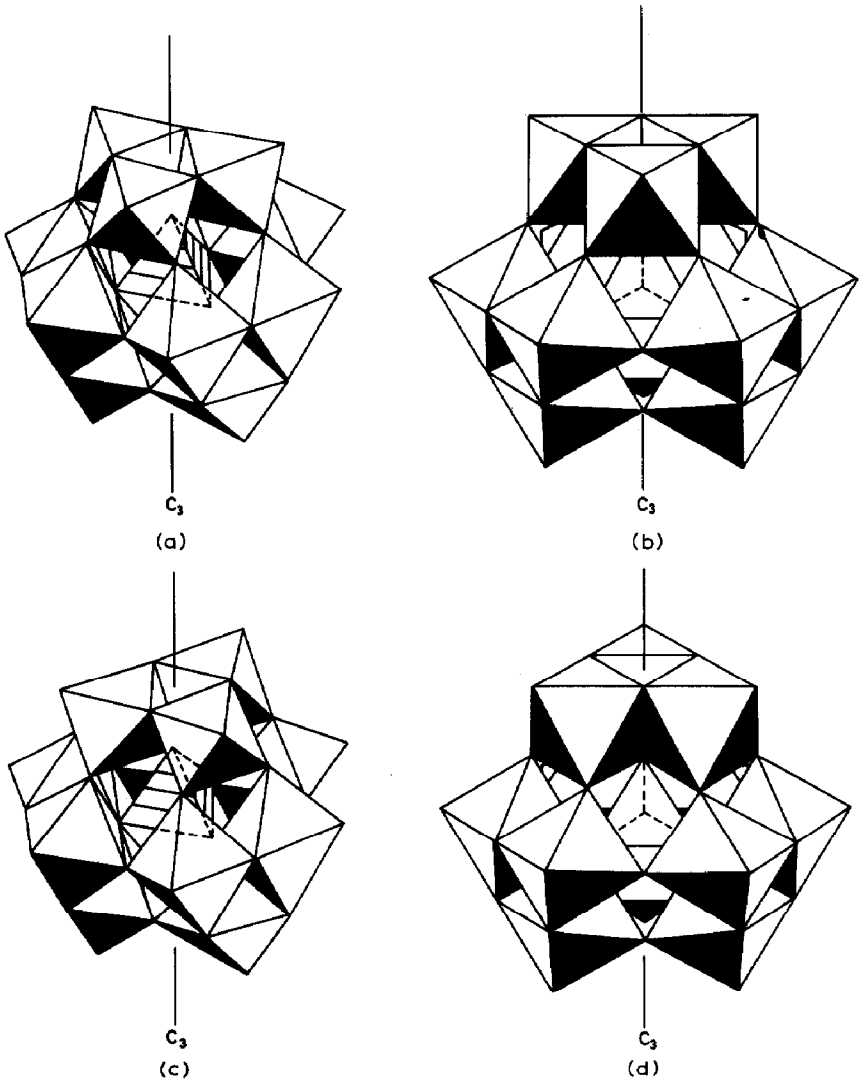

Fig. 1 (a, b) The α-Keggin structure $[X^{n+}Mo_{12}O_{40}]^{(8-n)-}$. (c, d) The β-Keggin structure.

spectra for both (unreduced) isomers are similar except for the higher extinction coefficients for the β-structures. For non-reduced Keggin ions the isomerisation always occurs from $\beta \rightarrow \alpha$. The rate of isomerisation can be slowed by using non-aqueous solvents; such media provide for a convenient synthesis of the β-isomer [19–22].

Keggin anions are quite compact but they can accommodate heteroatoms which differ considerably in size [23].

Partial hydrolysis of these anions in aqueous solution at pH ca. 5 yields the $[X^{n+}Mo_{11}O_{39}]^{(12-n)-}$ ion [9,10]. This complex is structurally related to

the α-Keggin anions. A defect α-Keggin structure results from the removal of a molybdenum atom and its terminal oxygen atom [24]. This also gives rise to the presence of *cis*-dioxo groups within the structure.

Divanadium-substituted Keggin anions were at one stage considered to have higher symmetry than their unsubstituted counterparts and to belong to the point-group O_h (the so-called pseudo-Keggin structure) [25]. However, this structural conclusion has since been shown to be based on a misinterpretation of the X-ray data, tetragonal species such as $[PV_2Mo_{10}O_{40}]^{5-}$ crystallising with normal Keggin structures, disordered as a whole in two positions related by a 90° rotation about the molecular $\bar{4}$ axis [25a].

The Dawson structure for octadecamolybdates, $[(X^{n+})_2Mo_{18}O_{62}]^{(16-2n)-}$

Anions of general formula $[(X^{n+})_2Mo_{18}O_{62}]^{(16-2n)-}$ are known to adopt one predominant isomeric form [16,26]. The A- and predominant B-isomers of the Dawson structure [16] are related to the Keggin anions. Pope [17] has recommended that the A- and B- labels should be replaced by β- and α- respectively and we will use these to describe the molybdate structures. The α-Dawson structure consists of two half-ions each of which is derived from the Keggin structure by removing three adjacent corner-linked octahedra, one from each of three edge-shared groups, as shown in Fig. 2. The two structural half units can be joined so that the octahedral vertices which were initially shared are shared again. The shared vertices lie in the equatorial mirror plane of the whole molecule, which has D_{3h} symmetry. The β-form is presumed to be analogous to that of $[P_2W_{18}O_{62}]^{6-}$, in which one group of three polar WO_6 octahedra has been rotated by 120° as in the β-Keggin structure. This isomer is centrosymmetric, with D_{3d} symmetry, and is less stable than the α-form because of internal strain within the molecule. The two main isomers for the Dawson structure are shown in Figs. 3a and 3b, there being a total of six possible isomers derivable by such 60° rotations [18].

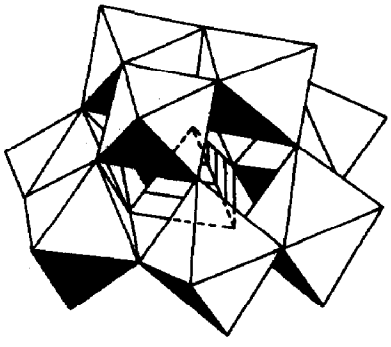

Fig. 2. The Dawson half-ion derived from the Keggin structure.

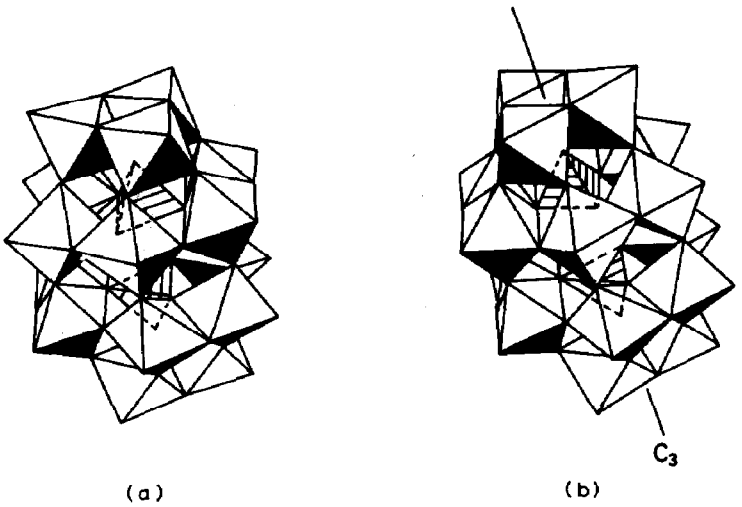

Fig. 3. (a) The α- (or B) Dawson structure, $[(X^{n+})_2Mo_{18}O_{62}]^{(16-2n)-}$. (b). The β- (or A) Dawson structure.

$[P_2Mo_{18}O_{62}]^{6-}$ has the α-Dawson structure (though distorted to D_3 rather than D_{3h} symmetry) and evidence has been found by Souchay et al. [27] for the unstable β-isomer in aqueous solution with X = P or As.

The $[(X^{n+})_2Mo_{17}O_{61}]^{(20-2n)-}$ ions are degradation products derived from the α-isomer in basic solutions. The structure has not yet been elucidated.

The Lindqvist–Aaronsson structure for hexamolybdates, $[Mo_6O_{19}]^{n-}$

The Lindqvist–Aaronsson polymolybdates of general formula $[Mo_6O_{19}]^{n-}$ have overall symmetry O_h. The octahedral structure consists of six edge-linked MoO_6 octahedra and consequently these anions contain only one type of linkage between octahedra. The structure is shown in Fig. 4.

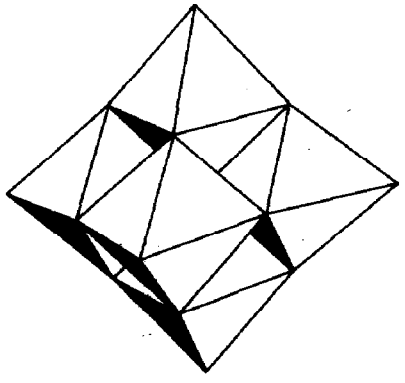

Fig. 4. The Lindqvist–Aaronsson structure, $[Mo_6O_{19}]^{n-}$.

Mono-vanadium substituted and one-electron reduced hexamolybdates have a pseudo-Lindqvist–Aaronsson structure [28] with C_{4v} symmetry.

C. RAMAN AND INFRARED SPECTRA OF POLYMOLYBDATES

(i) Hexamolybdates

The hexamolybdate anion, $[Mo_6O_{19}]^{2-}$, can be described as being octahedral with overall O_h symmetry, as above. The oxide cage contains three non-equivalent types of oxygen atom, one terminal, O_t, twelve bridging, O_b, and one central, O_c. There are also three non-equivalent Mo–O bonds, viz. $Mo{=}O_t$, $Mo{-}O_b$, and $Mo{-}O_c$. Although each molybdenum atom is displaced from the centre of its respective octahedron towards O_t, the tetragonal distortion is such that the overall O_h symmetry of the ion is preserved. Structural studies have, however, shown [29] that the symmetry of the anion is lower than O_h, namely C_i. For group-theoretical treatments the symmetry is more usually approximated to O_h.

A normal coordinate analysis of $[Mo_6O_{19}]^{2-}$ has been described by von Mattes [30] and Rocchiccioli-Deltcheff et al. [31]. The more reliable data are given by the latter authors as they include all of the internal coordinates in the calculation. Their methods are outlined below.

The $[Mo_6O_{19}]^{2-}$ ion has 69 normal modes of vibration and a group-theoretical analysis [30–32] reveals that there should be 11 Raman-active and 7 infrared-active fundamentals in the vibrational irreducible representation. i.e. for O_h symmetry,

$$\begin{aligned}\Gamma_{vib.} = {} & 3a_{1g}(\text{Raman}) + a_{2g}(\text{inactive}) + 4e_g(\text{Raman}) + 3t_{1g}(\text{inactive}) \\ & + 4t_{2g}(\text{Raman}) + a_{2u}(\text{inactive}) + e_u(\text{inactive}) \\ & + 7t_{1u}(\text{infrared}) + 4t_{2u}(\text{inactive}).\end{aligned}$$

11 Raman-active modes $(3a_{1g} + 4e_g + 4t_{2g})$
7 Infrared-active modes $(7t_{1u})$.

For the normal coordinate analysis performed by Rocchicciolli-Deltcheff et al. [31] the Wilson GF Matrix method [33] was used with 162 internal coordinates defined as:

6	$Mo{-}O_c$ bond stretches	c
6	$Mo{-}O_t$ bond stretches	t
24	$Mo{-}O_b$ bond stretches	b
12	$Mo{-}O_c{-}Mo$ angle bends	α
24	$O_c{-}Mo{-}O_b$ angle bends	β
24	$O_b{-}Mo{-}O_t$ angle bends	γ

24 O_b–Mo–O_b angle bends δ
12 Mo–O_b–Mo angle bends ϵ
6 torsional coordinates τ/c
(dihedral angles between planes having Mo–O_c as common line)
24 torsional coordinates τ/b
(dihedral angles between planes having Mo–O_b as common line)

The previous normal coordinate treatments of von Mattes et al. [30] and Farrell et al. [32] (for $[Nb_6O_{19}]^{8-}$ and $[Ta_6O_{19}]^{8-}$) ignored some of the internal coordinates such as MoO_cMo and MoO_bMo angle bends and torsional coordinates.

Of the seven predicted infrared bands six were observed (see Table 2). For the seventh an analogy was made with $[W_6O_{19}]^{2-}$ which has a band at 172 cm^{-1} which is weak and would probably not be observed for the molybdate. The Raman spectra were also lacking in bands but three polarised bands attributable to a_{1g} fundamentals were easily recognised. Of these two were assigned to pure stretching modes. The third (the middle band of the three) was broader and weaker than the other two, and thought to be part deformation in character. Buckley and Clark [34] have recently re-investigated the Raman spectrum of $[(C_4H_9)_4N]_2[Mo_6O_{19}]$ doped into KBr at 77 K. Three of the four missing predicted bands have been assigned by these authors. The full assignments and calculated band wavenumbers are compared with earlier work in Table 2. The assignments of Rocchicciolli-Deltcheff et al. [31] have been given using the internal coordinate notation and as a potential energy distribution (PED). Raman and infrared spectra for $[Mo_6O_{19}]^{2-}$ are also shown in Fig. 5.

The above treatment has been extended by the same authors to a normal coordinate analysis of isostructural mixed-valence and substituted (V^V) hexamolybdates [28]. One-electron reduced hexamolybdate $[Mo_6O_{19}]^{3-}$ has idealised C_{4v} symmetry [28] but the changes in bond lengths and bond angles on reduction are assumed to be small. Thus similar molecular parameters to those of $[Mo_6O_{19}]^{2-}$ can be used for the analysis. In turn the $[Mo_6O_{19}]^{2-}$ forcefield is assumed to be valid for the reduced analogue and an O_h model can be modified to take into account the observed splittings in the infrared spectrum. The splitting of bands is due to an actual lowering of the symmetry to C_{4v}. A consequence of this is that all of the modes which are inactive in O_h become active in C_{4v}. However, it was expected that only the modes allowed in O_h would give rise to intense bands; the modes inactive in O_h are unlikely to give rise to other than weak or unobservable bands in the spectra of C_{4v} symmetry species.

Of the bands observed in the infrared spectrum of $[Mo_6O_{19}]^{3-}$ (see Table 3 and Fig. 5) only that of highest wavenumber was not resolved into the a_1

TABLE 2

Calculated and observed wavenumbers (cm^{-1}) and assignments for the Raman and infrared spectra of $[Mo_6^{VI}O_{19}]^{2-}$

$T = 80$ K (i)	$T = 298$ K (ii)		$T = 298$ K (iii)		Symmetry and activity		Assignments as a PED and major component	
Obs.	Calc.	Obs.	Calc.	Obs.				
987	979	980	986	986	a_{1g}	R	93t	$\nu_s(Mo-O_t)$
965)								
954)	960	957	958	958	e_g	R	87t	$\nu_{as}(Mo-O_t)$
923)								
	954	951	956	956	t_{1u}	IR	93t	$\nu_{as}(Mo-O_t)$
810	799	809	817	817	e_g	R	$48b+18t+11\gamma$	$\nu_{as}(Mo-O_b)$
	796	798	795	796	t_{1u}	IR	$53b+13\gamma+11t$	$\nu_{as}(Mo-O_b)$
–	645	–	601	–	t_{2g}	R	$101\gamma+26b+6\epsilon$	$\delta(O_b-Mo-O_t)$
1597	558	580	598	598	a_{1g}	R	$42\gamma+23b+20\epsilon$	$\delta(O_b-Mo-O_t)$
	609	602	599	598	t_{1u}	IR	$78\gamma+30b$	$\delta(O_b-Mo-O_t)$
440	474	–	439	–	e_g	R	$61\gamma+59b+30\epsilon$	$\delta(O_b-Mo-O_t)$ + $\nu_{as}(Mo-O_b)$
	437	438	432	432	t_{1u}	IR	$40\gamma+13b+11\epsilon+8\delta$	$\delta(O_b-Mo-O_t)$
	349	356	351	352	t_{1u}	IR	$70c+8b$	$\nu_{as}(Mo-O_c)$
329	315	–	337	–	t_{2g}	R	$60\delta+6b+6\epsilon$	$\delta(O_b-Mo-O_b)$
286	264	278	285	285	a_{1g}	R	$80b+7c$	$\nu_s(Mo-O_b)$
	231	220	216	217	t_{1u}	IR	$170b+7\epsilon+6c$	$\nu_{as}(Mo-O_b)$
207	219	197	213	–	e_g	R	$79b+30\gamma+13c$	$\nu_{as}(Mo-O_b)$
200	182	163	206	205	t_{2g}	R	$58b+55\epsilon+29\delta$	$\nu(Mo-O_b)+\delta(Mo-O_b-Mo)$
	186	192	168	–	t_{1u}	IR	$150\delta+32c+14b+9\gamma$	$\delta(O_b-Mo-O_b)$
166	119	125	161	166	t_{2g}	R	$337b+20\delta+15\epsilon$	$\nu_{as}(Mo-O_b)$

(i) Raman spectrum recorded by Buckley and Clark [34] of $[(n\text{-}C_4H_9)_4N]_2[Mo_6O_{19}]$ as a KBr disc at ca. 80 K.

(ii) Data of von Mattes et al. [30]. Assignments have been slightly corrected to coincide with those of Rocchiccioli-Deltcheff et al. [31].

(iii) Data of Rocchiccioli-Deltcheff et al. [31]. Assignments are given as a potential energy distribution (PED) according to the method of Rocchiccioli-Deltcheff et al. [31], the nomenclature being explained in Section B.

and e components expected in C_{4v} symmetry; the rest had weak shoulders. Raman spectra were found to be difficult to obtain because of absorption of the laser beam (488.0 and 514.5 nm) and only low-intensity bands were observed. The normal coordinate analysis was then performed using a deficiency of observed band wavenumbers (compared with $[Mo_6O_{19}]^{2-}$), the force-field of the oxidised anion being used to initiate the calculation. The force-field of $[Mo_6O_{19}]^{3-}$ was considered to be that of $[Mo_6O_{19}]^{2-}$, modified to account for the observed splittings.

From the potential energy distribution (see Table 3) the high wavenumber

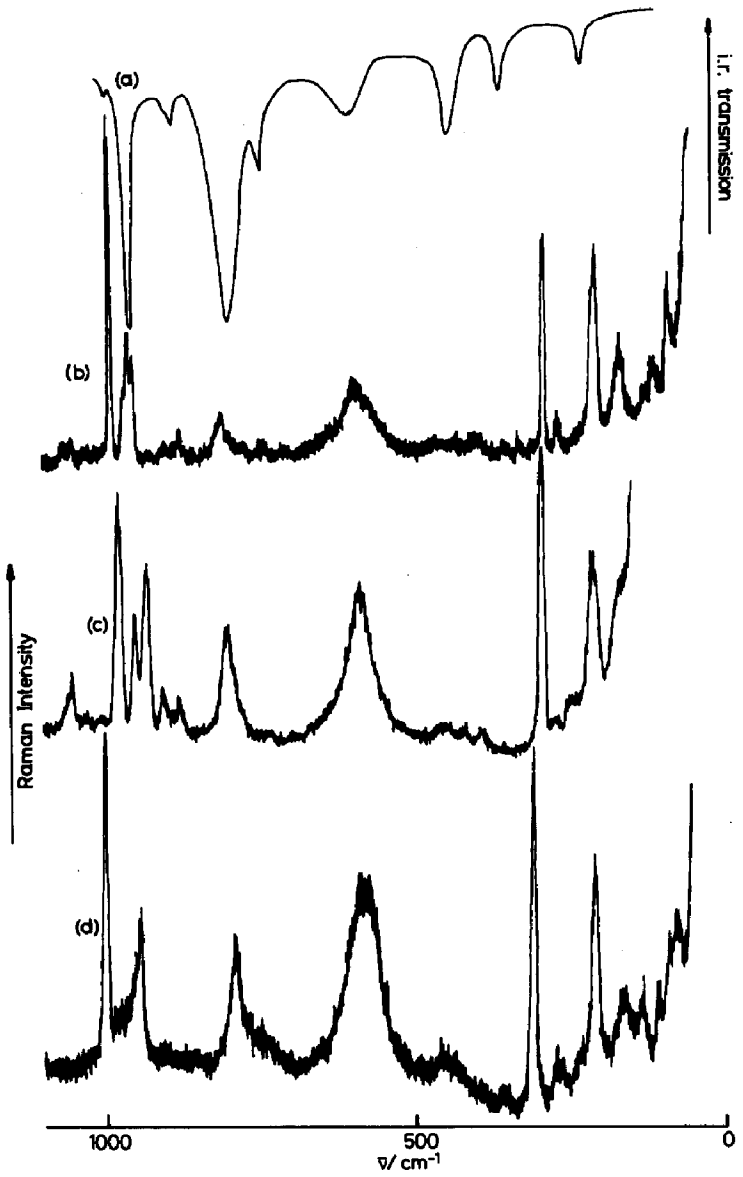

Fig. 5. Vibrational spectra of hexamolybdates. (a) Infrared spectrum of $[(n\text{-}C_4H_9)_4N]_2[Mo_6O_{19}]$ KBr disc. (b) Raman spectrum of $[(n\text{-}C_4H_9)_4N]_2[Mo_6O_{19}]$ KBr disc at ca. 80 K. (c) Raman spectrum of $[(n\text{-}C_4H_9)_4N]_3[V^VMo_5O_{19}]$ KBr disc at ca. 80 K. (d) Raman spectrum of $[CH_3NH_3]_2Na_2[V^{IV}Mo_5O_{19}]\cdot 6H_2O$ KBr disc at ca. 80 K. (a) Ref. 31, (b), (c), and (d) ref. 34.

mode at 986 cm^{-1} was the only one corresponding to a pure stretching vibration, i.e. $Mo{=}O_t$. All of the other bands were described as being due to mixed vibrations involving both stretching and bending. Many of the vibrations were found to involve $Mo{-}O_b$ but none can be described as a pure $Mo{-}O_b$ stretch.

TABLE 3

Calculated and observed wavenumbers (cm^{-1}) and assignments for the Raman and infrared spectra of one-electron reduced and vanadium-substituted hexamolybdates

(i)	(ii)	(iii)			Symmetry and activity		Assignment as a PED and major component [a]	
$[V^{V}Mo_5^{VI}O_{19}]^{3-}$ Obs.	$[V^{IV}Mo_5^{VI}O_{19}]^{4-}$ Obs.	$[Mo^{V}Mo_5^{VI}O_{19}]^{3-}$ Calc.	Obs.	Obsd. activity				
976	1006	970	970m	R	a_1	R,IR	70t + 22t′	ν_s(Mo–O_t)
949	957	937	937w	R	a_1	R,IR	86t	ν_s(Mo–O_t)
		937			b_1	R	83t	ν_{as}(Mo–O_t)
930	946	939	938vs	IR	a_1	R,IR	72t′ + 23t	ν_s(M*–O_t)
		939			e	R	90t	ν_{as}(Mo–O_t)
799	795	796	–		a_1	R,IR	44b + 19t + 11γ	ν(Mo–O_b)
		803	–		b_1	R	41b + 24t + 10γ	ν(Mo–O_b)
								ν(Mo–O_b)+
740	742	745	745sh	IR	a_1	R,IR	27b + 25b′ + 12γ + 6γ′	ν(M*–O_b)
775		783	780vs	IR	e	R,IR	41b + 13t + 12γ + 5b′	ν(Mo–O_b)
		–	–		b_2	R	–	
		–	–		e	R,IR	–	
		568	565m	IR	a_1	R,IR	67γ + 34b + 13γ′ + 12ε′	δ(O_b–Mo–O_t)
		616	615m	IR	e	R,IR	52γ′ + 35γ + 14b′ + 9ε′	δ(O_b–M*–O_t)
586	589	582	584w	R	a_1	R,IR	39γ + 21b + 13ε + 6ε′	δ(O_b – Mo–O_t)
		–	–		a_1	R,IR	–	
		–	–		b_1	R	–	

450	457	423	418s	IR	a_1	R,IR	$45\gamma + 24b + 11\epsilon + 5\delta$	$\delta(O_b\text{–}Mo\text{–}O_t)$
		449	450s	IR	e	R,IR	$45\gamma + 17b + 5b'$	$\delta(O_b\text{–}Mo\text{–}O_t)$
	363	342	343w	IR	a_1	R,IR	$40c + 26c' + 10b + 7\gamma' + 6\gamma$	$\nu(Mo\text{–}O_c)$
	353	358	358w	IR	e	R,IR	$66c + 15b + 7\gamma$	$\nu(Mo\text{–}O_c)$
		–	–		b_2	R	–	
		–	–		e	R,IR	–	
292	313	290	283vw		a_1	R,IR	$47b + 17b' + 6c$	$\nu(Mo\text{–}O_b)$
207	213	192	189w	IR	a_1	R,IR	$129b + 21c' + 17b' + 8\delta$	$\nu(Mo\text{–}O_b)$
		213	220w	IR	e	R,IR	$104b + 42b' + 12\delta' + 7\epsilon'$	$\nu(Mo\text{–}O_b)$
		–	–		a_1	R,IR	–	
		–	–		b_1	R	–	
		208	205vw	R	b_2	R	$32\delta' + 22\epsilon + 16\delta + 14b$	$\delta(O_b\text{–}M^*\text{–}O_b)$
		205			e	R,IR	$37\delta + 22\epsilon + 19b + 16\epsilon'$	$\delta(O_b\text{–}Mo\text{–}O_b)$
		132	–		a_1	R,IR	$232\delta + 142b + 20b' + 14\epsilon'$	$\delta(O_b\text{–}Mo\text{–}O_b)$
		154	150vw	IR	e	R,IR	$84b + 78\delta' + 72c + 59\delta + 7\gamma$	$\nu(Mo\text{–}O_b)$
163	165	63	–		b_2	R	$272b$	$\nu(Mo\text{–}O_b)$
		89	–		e	R,IR	$102b$	$\nu(Mo\text{–}O_b)$

[a] Internal coordinates and PED used as for Table 2. Internal coordinates involving Mo(V), V(V) or V(IV) are denoted by a prime (e.g. $t' = \nu(V^V\text{–}O_t)$).

(i) Raman spectrum recorded by Buckley and Clark [34] of $[(n\text{-}C_4H_9)_4N]_3[V^VMo_5O_{19}]$ as a KBr disc at ca. 80 K.

(ii) Raman spectrum recorded by Buckley and Clark [34] of $[CH_3NH_3]_2Na_2[V^{IV}Mo_5O_{19}]\cdot 6H_2O$ as a KBr disc at ca. 80 K.

(iii) Data of Rocchiccioli-Deltcheff et al. [28].

$M^* = Mo^{VI}$, V^V or V^{IV}.

The introduction of an electron which is localised on one molybdenum atom has a perturbing effect which weakens the $Mo^{V}=O_t$ bond, with respect to the $Mo^{VI}=O_t$ bonds, even though the latter are themselves somewhat weakened.

Raman spectra for V^{V} and V^{IV} substituted hexamolybdates have been reported by Buckley and Clark [34]. The spectra of the unsubstituted and substituted species were very similar to one another, apart from a well-resolved band at ca. 930 cm^{-1} for $[VMo_5O_{19}]^{3-}$. This band is due to ν(V=O) and it also appears as a less well resolved shoulder in the spectrum of the V^{IV} substituted analogue. The $[VMo_5O_{19}]^{4-}$ ion also shows resonance enhancement of certain bands (see section B (iii)). The conclusion is that no great structural change occurs on substitution and subsequent reduction (see Fig. 5).

Recent theoretical treatments of mixed-valence complexes [35,36] have been developed to produce potential energy surfaces. These are in turn used to describe thermal and optical electron transfers and to calculate inter-valence charge-transfer band contours [35,36]. Rocchicciolli-Deltcheff et al. [28] point out that the theories assume two points: that the force constants relating to stretching metal–ligand bonds are the same for both oxidised and reduced forms of the complexes and that the normal mode along which electron transfer occurs is a pure stretching vibration.

(ii) Dodecamolybdates

Vibrational studies on dodecamolybdates have been carried out by several groups and some tentative assignments have been given. Work published prior to 1970 related to vibrational investigations at wavenumbers only greater than 300 cm^{-1} [37–40] and interpretations were made by assuming that the anions could be separated into indepedent parts [38,39]. The XO_4 unit at the centre of the anion was assumed to vibrate independently of the surrounding MoO_6 octahedra [39]. The possibility of coupling between vibrations was not envisaged and consequently assignments were often wrong and differed from one another.

More recent investigations by Rocchicciolli-Deltcheff et al. [41–43] and Lyhamm et al. [44–48] have been more successful and their collected publications provide two methods for interpreting the vibrational spectra of dodecamolybdates. Yurchenko and Bugaev [59] have also calculated vibrational wavenumbers for $[PMo_{12}O_{40}]^{3-}$.

Rocchicciolli-Deltcheff et al. [41–43] treat the molecule as a whole and provision is made for mixing between symmetry coordinates. Conversely, Lyhamn et al. [44–48] tackle the problem by assuming that the α-Keggin structure can be divided into four Mo_3O_7 units which act as "ligands" to the

central X atom. The vibrations of each unit are treated separately. The two methods are outlined below:

The $[X^{n+}Mo_{12}O_{40}]^{(8-n)-}$ ion, in isolation, has T_d symmetry and consists of the central XO_4 unit surrounded by twelve distorted MoO_6 octahedra, each of C_s symmetry (cf. $[Mo_6O_{19}]^{2-}$). The octahedra form trimeric Mo_3O_{13} groups each of which has C_{3v} symmetry. Within the overall structure four inequivalent types of oxygen atom can be envisaged [41]:

4 O_a: each shared by XO_4 and three octahedra from the same Mo_3O_{13} group.
12 O_b: Mo–O_b–Mo bridges between different Mo_3O_{13} groups.
12 O_c: Mo–O_c–Mo bridges within the same Mo_3O_{13} group.
12 O_t: Mo–O_t terminal oxygen atoms.

An isolated $[X^{n+}Mo_{12}O_{40}]^{(8-n)-}$ molecule gives rise to the following vibrational irreducible representation [41–49]:

$$\Gamma_{vib} = 9a_1 + 4a_2 + 13e + 16t_1 + 22t_2$$

i.e. 44 Raman bands ($9a_1 + 13e + 22t_2$)
22 infrared bands ($22t_2$ coincident with $22t_2$ Raman bands).

Using internal coordinates (i.e. bond lengths and angles) there are 72 Mo–O bonds, 4 X–O bonds, 144 $OM\hat{o}O$ angles and 6 $O\hat{X}O$ angles.

For the Mo–O and X–O bonds one can derive:

$$\Gamma_{Mo-O} = 4a_1 + 2a_2 + 6e + 8t_1 + 10t_2$$

which can be separated out according to oxygen atom type:

$$\Gamma_{Mo-O_a} = \Gamma_{Mo-O_d} = a_1 + e + t_1 + 2t_2$$

$$\Gamma_{Mo-O_b} = \Gamma_{Mo-O_c} = a_1 + a_2 + 2e + 3t_1 + 3t_2$$

and

$$\Gamma_{X-O} = a_1 + t_2$$

Therefore, for internal vibrations:

$$\Gamma_\nu = 5a_1 + 2a_2 + 6e + 8t_1 + 11t_2.$$

For the $OM\hat{o}O$ and $O\hat{X}O$ angles we have:

$$\Gamma_{OM\hat{o}O} = 7a_1 + 5a_2 + 12e + 17t_1 + 19t_2$$

$$\Gamma_{O\hat{X}O} = a_1 + e + t_2$$

Therefore, for the internal angle deformations we have:

$$\Gamma_\delta = 8a_1 + 5a_2 + 13e + 17t_1 + 20t_2$$

However, these representations contain the following redundancies:

$$4a_1 + 3a_2 + 6e + 9t_1 + 9t_2$$

Assignment of the above to the vibrational modes is not obvious but an a_1 active vibration is easily envisaged as an in-phase motion of all of the terminal oxygen atoms outwards from the molybdenum atoms. An out-of-phase movement would have e or t_2 symmetry. The Mo–O_a bonds are quite long and the XO_4 tetrahedron is assumed, to a first approximation, to vibrate independently of the rest of the ion. This gives rise to two infrared-active t_2 modes (ν(X–O) and δ(O–X–O)) and two additional Raman-active vibrations of a_1 symmetry. The Mo–O_b and Mo–O_c vibrations are difficult to separate and much mixing occurs between them. Analogous arguments to those above can also be applied to the angle deformation modes, O_t–Mo–O_b and O_t–Mo–O_c.

The method of Lyhamn et al. [44–48] divides the α-Keggin molecule into separate units and analyses the vibrations of each. Four Mo_3O_7 units, each of C_{3v} symmetry, act as "ligands" (not in the chemical sense but more as an aid to mathematics). This method is analogous to the vibrational analysis of complexes of the type $Ni(PF_3)_4$ [50], with added features such as linking of the ligands with bridges thus giving rise to "interligand vibrations". These vibrations also include "interligand couplings". The Mo_3O_7 "ligands" themselves can be further divided into smaller parts. These and the interligand Mo_3O_{13} units along with their structural relationship to the XO_4 tetrahedron are shown in Fig. 6. The numbering system used for the normal coordinate analysis is also shown in the diagram.

The Mo_3O_7 unit has 24 normal modes of vibration in C_{3v} symmetry, i.e.

$$\Gamma_{Mo_3O_7} = 6a_1 + 2a_2 + 8e$$

For the whole complex (T_d symmetry) one obtains 96 ligand vibrations by correlating C_{3v} with T_d, i.e.

$$\Gamma_{(T_d)} = 6a_1 + 2a_2 + 8e + 10t_1 + 14t_2$$

This representation is the distribution of the ligand modes in T_d symmetry. For the "interligand" vibrations involving Mo_3O_{13} units, nine modes can be considered.

$$\Gamma_{Mo_3O_3} = 2a_1 + a_2 + 3e$$

This representation, in turn, gives rise to 36 "interligand" modes for the whole complex.

$$\Gamma_{(T_d)} = 2a_1 + a_2 + 3e + 4t_1 + 5t_2$$

The total of 153 normal modes of vibration for the whole complex is

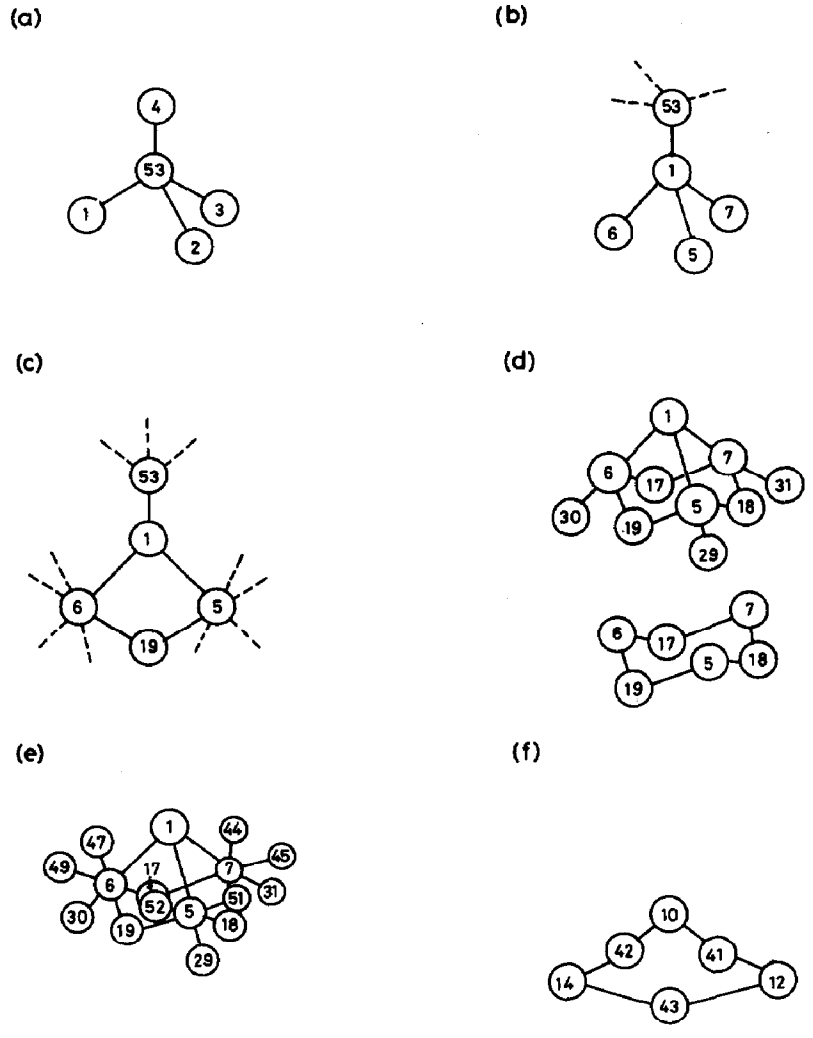

Numbering of atoms in $PMo_{12}O_{40}$

LIGAND	A	B	C	D	
	1	2	3	4	O atoms arranged tetrahedrally
	5	8	11	14	
	6	9	12	15	Mo atoms
	7	10	13	16	
	17	20	23	26	
	18	21	24	27	O atoms in Mo_3O_{13} rings
	19	22	25	28	
	29	32	35	38	
	30	33	36	39	other O atoms
	31	34	37	40	
	41	44	47	50	bridging O atoms in interligand
	42	45	48	51	structures
	43	46	49	52	
		53			P atom

Fig. 6. The numbering of the atoms of the PO_4 unit of $[PMo_{12}O_{40}]^{3-}$ and the molecular fragments as used by Lyhamn et al. [45] for the normal coordinate analysis of this anion. (a) Tetrahedral PO_4 unit. (b) $POMo_3$ unit. (c) $POMo_2O$ unit with a four membered Mo_2O_2 ring. (d) Mo_3O_7 unit with a Mo_3O_3 ring. (e) Mo_3O_{13} unit. (f) Mo_3O_3 ring made up from "interligand" bonds.

distributed as follows:

$$\Gamma_{vib.} = 9a_1 + 4a_2 + 13e + 16t_1 + 22t_2$$

This result is identical with that obtained using the previous method by Rocchicciolli-Deltcheff et al. [41–43] and Kasprzak et al. [49].

In order to attempt as complete an assignment as possible, Lyhamn et al. [45] carried out a force-field calculation, using the G-F matrix method [33], and also determined sets of symmetry coordinates for individual units and the whole molecule.

The calculated wavenumbers and assignments of Lyhamn et al. [45] and Yurchenko and Bugaev [59] do not agree. However those of Lyhamn et al. do show a reasonable agreement with experiment for $[PMo_{12}O_{40}]^{3-}$ [34] and the calculated and experimental wavenumbers for this and other dodecamolybdates are shown in Table 4. The assignments for ν_s(P–O) and ν_s(Mo–O_t) are also at variance with those of Rocchicciolli-Deltcheff et al. [41,42] in the high wavenumber region. It also appears that the earlier assignments, such as those of Lange et al. [39], are also in error. The assignment of Rocchiccioli-Deltcheff et al. for ν_s(Mo–O_t) at ca. 990 cm^{-1} does, however, seem to be correct. Vibrational spectra are shown in Fig. 7.

The results of both of the above methods show that some of the predicted infrared and Raman bands are missing. This is probably due to the weakness of the bands.

The β-Keggin isomer has C_{3v} symmetry by virtue of the rotation of one Mo_3O_{13} group by 60° about a C_3 axis of the α-isomer. The vibrational irreducible representation for this structure can easily be derived by using correlations between the point-groups T_d and C_{3v} [49].

$$\Gamma_{vib} = 31a_1 + 20a_2 + 51e$$

i.e. 82 coincident Raman and infrared bands. Splitting of the α-Keggin structure into units can be of use in assigning group frequencies to parts such as Mo_3O_6, etc. [19,49]. These characteristic frequencies can be used to distinguish between the spectra of the α- and β-Keggin anions. The spectra should differ only in the spectral regions which are characteristic of "interligand vibrations" [19]. This approach has been used by Thouvenot et al. [19] and Kasprzak et al. [49] to investigate structural isomerism in $[X^{n+}Mo_{12}O_{40}]^{(8-n)-}$, where $X = Si^{IV}$, Ge^{IV}, P^V or As^V. A good correlation was found between vibrational and structural data.

The main differences between the vibrational spectra of the α- and β-isomers are found in the fact that, by changing the symmetry from $T_d(\alpha)$ to $C_{3v}(\beta)$, the sixteen inactive t_1 modes for the former become both infrared and Raman allowed via their e components for C_{3v} symmetry [19,49]. The vibrations affected by the rotation of the Mo_3O_{13} relate to the Mo–O–Mo

TABLE 4

Calculated and observed wavenumbers (cm^{-1}) and assignments for the Raman and infrared spectra of dodecamolybdates

(a) Dodecamolybdates [a]

α-$[SiMo_{12}O_{40}]^{4-}$		$[GeMo_{12}O_{40}]^{4-}$		α-$[PMo_{12}O_{40}]^{3-}$		$[AsMo_{12}O_{40}]^{3-}$		Assignment
IR	R	IR	R	IR	R	IR	R	
				1063				ν_{as}(P–O)
985		960				980		
	967.5 *		967.5 *		986 *		986 *	ν_s(Mo=O_t)
							968	
945)					971)			
940)	941.5	939	940	965	964)	965	961	ν_{as}(Mo=O_t)
				955				
899								ν_{as}(Si–O)
						895		ν_{as}(As–O)
		880						
868	883.5	873	875	880	894	855	880	ν_{as}(Mo–O_b–Mo)
		812						ν_{as}(Ge–O)
795		778		805		790		ν_{as}(Mo–O_c–Mo)
							773	
	686		684				655	
635		635		612		608		
600		600						
	620.5 *		621 *		603 *		602 *	ν_s(Mo–O_c–Mo)
532								
509		507		505		498		
463	465	465	465	464	465	470	488	
452		449	455		451	453	454	
397							397	
380	371	377	388	386	370	379	385	
			359					
340	344	330	339	340		330		
			331					
282	290	290			255			
	246.5 *		247 *		246 *		247 *	ν_s(Mo–O_a)
			232				230	
	208.5		211		215		214	
			206		203		203	
			186					
	167		166		169			
	156		156		154		157	
	109.5		109		109		112	
	88		91		84		83	
	64		64					

TABLE 4 (continued)
(b) Calculated and observed wavenumbers (cm^{-1}) for $[PMo_{12}O_{40}]^{3-}$

(i)			(ii)				(iii)
Calc.	Symmetry	Activity	Calc.	Symmetry	Activity	Tentative assignment	Observed at ca. 80 K
1151	t_2	R,IR	1107	t_2	R,IR	ν_{as}(P–O)	1118
1057	a_1	R	980	a_1	R	ν_s(P–O)	992
994	t_2	R,IR	975	t_2	R,IR		
995	a_1	R	974	e	R	ν_{as}(Mo–O_t)	
991	t_2	R,IR	970	t_2	R,IR		971
990	e	R	958	a_1	R	ν_s(Mo–O_t)	
945	e	R	945	e	R	ν_{as}(Mo–O_a)	897
946	t_2	R,IR	941	t_2	R,IR		
894	t_2	R,IR	885	t_2	R,IR		880
894	e	R	883	e	R		
867	t_2	R,IR	799	t_2	R,IR	ν(Mo–O_b)	779.5
800	e	R	768	e	R		747
730	t_2	R,IR	688	a_1	R	ν_s(Mo–O)	700
711	e	R	688	t_2	R,IR		
700	a_1	R	678	t_2	R,IR		664.5
670	t_2	R,IR	675	e	R		
610	t_2	R,IR	582	a_1	R		607
600	a_1	R	571	t_2	R,IR		592
596	e	R	549	t_2	R,IR		
592	t_2	R,IR	547	e	R		
501	a_1	R	546	a_1	R		
496	t_2	R,IR	528	t_2	R,IR		504
438	a_1	R	469	t_2	R,IR		469
437	t_2	R,IR	466	t_2	R,IR		
411	t_2	R,IR	463	e	R		
391	e	R	452	a_1	R		
391	t_2	R,IR	422	t_2	R,IR		407
349	e	R	358	t_2	R,IR		374
340	t_2	R,IR	327	t_2	R,IR		345
305	t_2	R,IR	316	e	R		
298	a_1	R	309	a_1	R		
262	a_1	R	296	e	R		
233	t_2	R,IR	284	t_2	R,IR		286.5
215	e	R	269	t_2	R,IR		
204	t_2	R,IR	249	e	R		
186	e	R	240	a_1	R		254
186	t_2	R,IR	233	t_2	R,IR		245
159	t_2	R,IR	219	t_2	R,IR		225
149	e	R	206	a_1	R		212
146	t_2	R,IR	205	e	R		
124	e	R	197	t_2	R,IR		199
91	e	R	174	e	R		180

TABLE 4 (continued)

(i)			(ii)				(iii)
Calc.	Symmetry	Activity	Calc.	Symmetry	Activity	Tentative assignment	Observed at ca. 80 K
91	t_2	R,IR	170	t_2	R,IR		160
89	a_1	R	154	e	R		108
							81

[a] Data of Rocchiccioli-Deltcheff et al. [21]. Raman and infrared spectra recorded as solids at room-temperature.

* Polarised in DMF solution.

(i) Data of Yurchenko and Bugaev [59].

(ii) Data of assignments of Lyhamn et al. [45]. These assignments are at variance with those of Rocchiccioli-Deltcheff et al. [41] and are discussed in the text.

(iii) Raman spectrum of $[(C_4H_9)_4N]_3[PMo_{12}O_{40}]$ recorded as a KBr disc at ca. 80 K by Buckley and Clark [34].

bridges spanning two different groups. The characteristic bands for these vibrations appear below 300 cm^{-1} and the β-isomer is expected to show more bands in this region [49]. The detailed treatment of the α-isomer by Lyhamn (described above) does not, unfortunately, distinguish between vibrations between Mo_3O_{13} groups and those within a single group. Kasprzak et al. [49] claimed to have observed new Raman bands at 148 and 191 cm^{-1} assigned to β-$[SiMo_{12}O_{40}]^{4-}$. This classical approach has been questioned by Thouvenot et al. [19] and Buckley and Clark [34] as they failed to observe the low-energy vibrational bands due, supposedly, to the β-isomer. The concept of group frequencies was again used by these authors and the low-wavenumber region was studied in detail. In this region both "ligand" vibrations (due to Mo_3O_6) and "interligand" vibrations (i.e. ν(Mo–O_b–Mo)) occur. The twelve O_b atoms described earlier link the trimeric units and it was considered more judicious to look at vibrations involving these atoms. Small but significant changes in the Raman and infrared spectra occur in this region and these are sufficient to differentiate between α- and β-structures. It was also found by Thouvenot et al. [19] that both α- and β-structures exist holds for X = Si and Ge but only the α-form for X = P and As. The different charge distribution due to P^V or As^V destabilises the β-structure with respect to either the α-isomer or some other structure [19]. It is also known that the β-Keggin isomers are less stable with respect to reduction than are the α-isomers. Vibrational wavenumbers characteristic of dodecamolybdates are shown in Table 5. These quantities are quite dependent upon the nature of the counterion, X, and α–β isomerism [19,49,51]. Of the characteristic wavenumbers only ν(Mo=O_t) is a pure stretching vibration, the others are all mixed.

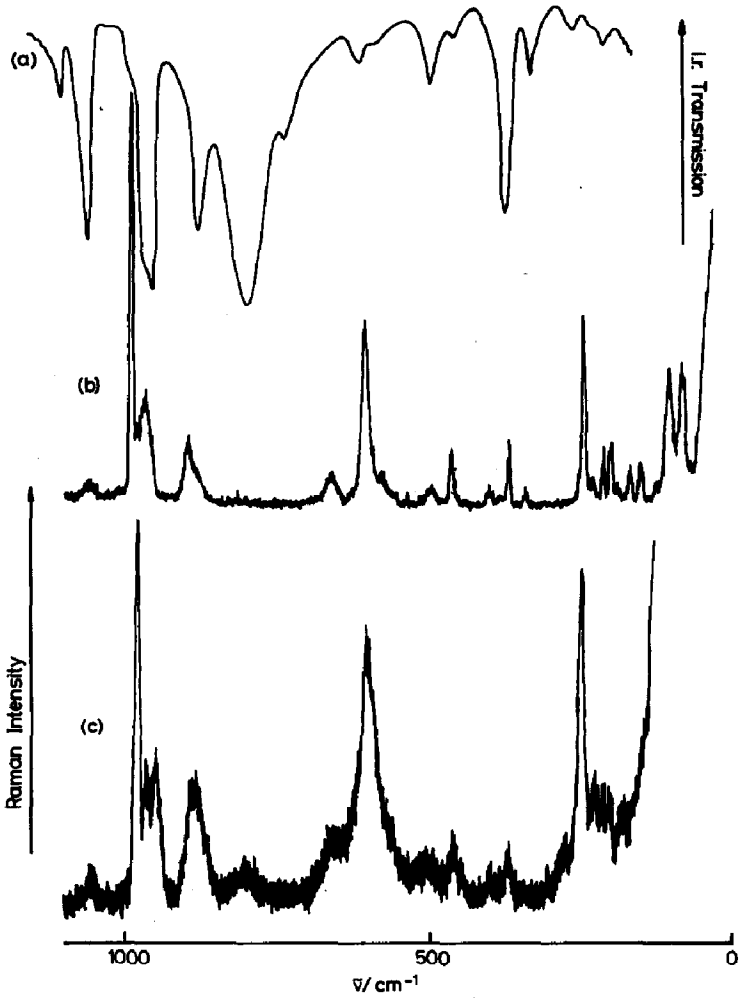

Fig. 7. Vibrational spectra of dodecamolybdates. (a) Infrared spectrum of α-[(n-$C_4H_9)_4N]_3[PMo_{12}O_{40}]$ KBr disc. (b) Raman spectrum of $[(n\text{-}C_4H_9)_4N]_3[PMo_{12}O_{40}]$ KBr disc at ca. 80 K. (c) Raman spectrum of $[(n\text{-}C_4H_9)_4N]_4[PV^VMo_{11}O_{40}]$ KBr disc at ca. 80 K. (a) Ref. 21, (b) and (c) Ref. 34.

Anion–anion interactions and their effect on the vibrational spectra of dodecamolybdates have been investigated by Rocchicciolli-Deltcheff et al. [21].

(iii) Reduced dodecamolybdates

Infrared studies of reduced dodecamolybdates have been carried out by, amongst others, Akimoto and Echigoya [52], Tsai et al. [53], Tsuneki et al. [54], Mizuno et al. [55], and Tarasova et al. [51].

TABLE 5

Characteristic or group-wavenumbers (cm^{-1}) for hexa- and dodeca-molybdates

	ν_{as}(X–O) [a]	ν_s(Mo=O_t)	ν_{as}(Mo=O_t)	ν_{as}(Mo=O_t)	ν_s(Mo–O_c–Mo)	ν_{as}(Mo–O_c–Mo)	ν_{as}(Mo–O_b–Mo)	ν_{as}(Mo–O_b–Mo)	ν_s(Mo–O_b)
	IR	R*	R	IR	R*	IR	R*	IR	R*
Dodeca-	890–1065	965–990	940–970	940–965	600–630	770–805	820–910	855–885	244–247
Hexa-	–	980–986	920–965	950–956					265–285

[a] X denotes the heteroatom.

The mechanism of reduction of $[PMo_{12}O_{40}]^{3-}$ [52–55] and $[SiMo_{12}O_{40}]^{4-}$ [52] by organic compounds [53,54], by H_2 [55], and electrolytically [52], has been investigated using the intensities of four infrared bands as an indicator. The four bands used were ν(P–O) at 1060 cm^{-1}, $\nu(Mo{=}O_t)$ at 960 cm^{-1}, δ(Mo–O–Mo) at 880 and 790 cm^{-1} [52–55], and δ(O–X–O) where X = P or Si [52].

Electrolytic reduction of ammonium salts of $[PMo_{12}O_{40}]^{3-}$ and $[SiMo_{12}O_{40}]^{4-}$ in two-electron steps was investigated by Akimoto and Echigoya [52]. A two-electron reduction step for both molybdates caused a decrease in the intensity of ν(X–O) and δ(Mo–O–Mo) but the $\nu(Mo{=}O_t)$ band was unaffected. The wavenumbers of the two former bands were also red shifted. A more significant decrease in intensity was seen when a further two-electron step was induced and both ν(X–O) and ν(Mo–O–Mo) virtually disappeared. The decrease in intensity was explained by the lowering of the overall symmetry of the molecule due to the introduction of Mo(V). It was also concluded that the bridging oxygen atoms did not participate in the reduction.

Similar observations were made by Tsai et al. [53], who monitored the effects induced in the infrared spectrum by reducing $[PMo_{12}O_{40}]^{3-}$ with ethyl methyl ketone, crotonaldehyde, methacrylaldehyde, 1-butene, and 1,3-butadiene. They also noted that the intensities of the same bands decreased as the reaction temperature was raised. This was interpreted as the effect of the water of hydration on the reduction process.

The reduction of $[PMo_{12}O_{40}]^{3-}$ with H_2 has also been investigated [54,55] and changes similar to those above were again found in the infrared spectrum. The intensities were again attributed to the lowering of symmetry by the introduction of a Mo^V centre.

Few Raman spectra of reduced dodecamolybdates have been reported in the literature, the work of Kasprzak et al. [49] and Buckley and Clark [56] providing the only examples. The Raman spectrum of a partially reduced dodecamolybdate, β-$[SiMo_{12}O_{40}]^{4-}$, has been observed by Buckley and Clark [56]. The reduced species was obtained by irradiating a sample of the dimethylammonium salt suspended in petroleum ether with ultraviolet light. The Raman spectrum was recorded with a laser line of wavelength well removed from that of any absorption bands of the complex in order to avoid resonance effects (see later); it was found to be virtually identical with that of the unreduced salt. This obviously implies that the partially reduced species retains the Keggin structure after reduction. Tarasova et al. [51] have detected differences between the infrared spectra of reduced α- and β-silicomolybdic acids.

Mixed-valence dodecamolybdates can be modelled using V^{IV}-substituted analogues [34,57,58]. These systems have been investigated by the above

authors and by Yurchenko [25,59]. Kasprzak et al. [49] modelled the reduced dodecamolybdates using V^V-substituted compounds such as $[PV_2Mo_{10}O_{40}]^{5-}$, $[PV_3Mo_9O_{40}]^{7-}$, etc. (see next section). However, these complexes are isoelectronic with the fully oxidised species and do not show mixed-valence character. There is no possibility of electron transfer between V^V and Mo^{VI} as neither ion possesses a *d*-electron. A more valid analogy would have been made by using V^{IV}, which is isoelectronic with Mo^V. The V^{IV}-substituted compounds also show intense intervalence charge-transfer transitions in their electronic spectra. Kasprzak et al. [49] also studied solutions of $[PMo_{12}O_{40}]^{5-}$ as well as further (electrolytically) reduced dodecamolybdates in 1:1 H_2O : 1,4-dioxan. Difficulty was found by these authors in recording Raman spectra because of absorption of the laser beam by the sample. The resonance Raman effect [60] was then supposedly utilised to obtain Raman spectra. It was claimed that spectra were observed by way of resonance enhancement of the vibrational modes using exciting radiation of wavelength 514.5 nm. As will be shown later this is clearly not the case and instead only a normal Raman spectrum could be recorded with this exciting line (see section C, resonance Raman spectra of reduced molybdates).

(iv) Vanadium-substituted dodecamolybdates

Vanado-substituted dodecamolybdates have been investigated by Kasprzak et al. [49], Yurchenko and Bugaev [25,59], Tsigdinos and Hallada [61], and Buckley and Clark [34]. As indicated in the previous section vanadium(IV)-substituted molybdates can be used to model the electronic properties of mixed-valence molybdenum blues. The vanadium(V) analogues, although isoelectronic with the fully oxidised molybdates, can also give useful spectroscopic information. The splitting of bands and the introduction of new bands in infrared and Raman spectra induced by substitution can be of use in assigning vibrational modes. Both V^{IV}- and V^V-substituted $[PMo_{12}O_{40}]^{3-}$ have been studied by Yurchenko [25], Buckley and Clark [34], and Kasprzak et al. [49] (see previous section).

Buckley and Clark [34] have investigated the effect of V^V substitution on the Raman spectrum of $[PMo_{12}O_{40}]^{3-}$. The only apparent difference is the appearance of a new band at ca. 930 cm^{-1} due to $\nu(V{=}O)$. The overall appearance of the spectra is unchanged on substitution, showing that very little or no change in structure had occurred (see Fig. 7).

Yurchenko [25] and Kasprzak et al. [49] have reported Raman and infrared spectra for anions of the type $[P(V^V)_nMo_{12-n}O_{40}]^{(3+n)-}$, where $n = 0$–3, both as solids and in solution. Yurchenko [25] has also found that increasing n, the number of vanadium atoms in the complex, has the same effect on the Raman spectra of the compounds in solution as increasing the

pH. Comparisons were made between solids and solutions of samples with $n = 0$–9. Differences between spectra were found to be only slight. The spectra were also similar to those for protonated dodecamolybdophosphate at pH 1.2 and the sodium salt in the solid state. As for the infrared spectra recorded by Yurchenko [25], the intensity of ν(M=O) at 960 cm^{-1} was found to fall as n was increased. Changes were also observed in other regions of the spectrum where bands grew in intensity (760–780 cm^{-1} and 930–940 cm^{-1}). This behaviour was interpreted in terms of the appearance of ν(V=O) at 930 cm^{-1} and δ(V–O–V) at 760–780 cm^{-1}. V^{IV}-substituted molybdates were briefly studied by Yurchenko [25] and their conclusion, drawn from infrared and X-ray studies, was that very little structural change occurred on reduction.

Kasprzak et al. [49] reported Raman spectra for aqueous solutions of vanadomolybdates where $n = 1$–3. The spectra were all identical and it was found that ν(V=O) was obscured by ν_{as}(Mo–O_t) at 972 cm^{-1}, in contrast to the resolved bands seen by Yurchenko [25] and Buckley and Clark [34]. ν_{as}(Mo=O_t) was also reported to be less well resolved from a band at 995 cm^{-1}, assigned to ν(P–O), than in the unsubstituted molybdate. This assignment seems to be in error and the band is more likely due to ν_s(Mo=O_t). The vanadomolybdates were also found to absorb the exciting radiation when laser lines at 488.0 and 514.5 nm were used. Similar Raman and infrared spectra have been reported for these compounds by Ai et al. [62]. The masking of ν(V=O) by ν(Mo=O) has also been observed in infrared spectra by Tsigdinos and Hallada [61].

The main features of the vibrational spectra of vanadomolybdates are, along with the characteristic bands of the unsubstituted anion, new bands in the regions 750–800 and 900–980 cm^{-1} due to δ(V–O–V) and ν(V=O), respectively. Band wavenumbers are given in Table 6.

(v) Octadecamolybdates

Very little has appeared in the literature on vibrational studies on octadecamolybdates. Although the structure of $[P_2Mo_{18}O_{62}]^{6-}$ is well characterised [26], a normal coordinate analysis and assignments of vibrational spectra have yet to appear. Lyhamn and Pettersson [63,64] recorded the infrared [63] and Raman [64] spectra of $[P_2Mo_{18}O_{62}]^{6-}$ species but they drew few structural conclusions. Problems associated with sample reduction and decomposition by the laser beam were encountered when recording Raman spectra [64]. Consequently, little information was obtained from the spectra of crystalline samples and so solution work was carried out. The spectra seemed to be characterised by two intense peaks at 730 and 978 cm^{-1}. These bands were not assigned but, by analogy with those observed for dodecamo-

TABLE 6

Observed wavenumbers (cm^{-1}) and assignments for the Raman and infrared spectra of vanadium(V)-substituted dodecamolybdates

$[PV^{V}Mo_{11}^{VI}O_{40}]^{4-}$			$[PV_2^{V}Mo_{10}^{VI}O_{40}]^{5-}$		$[PV_3^{V}Mo_9^{VI}O_{40}]^{6-}$		Assignment
R(80 K) [a]	R [b]	IR [c]	R [b]	IR [c]	R [b]	IR [c]	
		1060		1100		1100	$\nu_{as}(P-O)$
980	995		992		992		$\nu_s(Mo=O_t)$
972	972		972		973		$\nu_{as}(Mo=O_t)$
951							$\nu(V=O_t)$
889	897	890	896	860	892	875	$\nu_{as}(Mo-O_b-Mo)$
866		830-		820-		830-	bridging vibrations [b]
807		700		700		710	(IR only)
656	649		657		–		
603	605		608		607		$\nu_s(Mo-O_c-Mo)$
572							
496							
463	451		453		450		
423							
373	378		382		–		
253	250		252		255		$\nu_s(Mo-O_a)$
231							
216	214		213		213		
207							
183	155		154		156		
123							
111	105		105		108		
89							

[a] Raman spectrum of $[(n\text{-}C_4H_9)_4N]_4[PVMo_{11}O_{40}]$ recorded as a KBr disc at ca. 80 K by Buckley and Clark [34].

[b] Infrared spectra of solid acid hydrates recorded by Tsigdinos and Hallada [61].

[c] Raman spectra of aqueous solutions recorded by Kasprzak et al. [49].

lybdates, they seem to be due to δ(Mo–O–Mo) and ν(Mo–O), respectively.

Infrared spectra were also recorded [63] but only general assignments were given and simple comparisons between spectra were made. The band wavenumbers (infrared and Raman) and general assignments are shown in Table 7.

D. ELECTRONIC STRUCTURES OF REDUCIBLE HETERO- AND ISOPOLYMOLYBDATES

Following the classification by Pope [7] and Nomiya and Makoto [8] described in section B(i) one can readily see the implications for electronic

TABLE 7

Observed wavenumbers (cm^{-1}) and assignments for the Raman and infrared spectra of octadecamolybdates

$Na_6[P_2Mo_{18}O_{62}]\cdot 24H_2O$			Assignment
IR(s) [a]	R(s) [b]	R(aq) [b]	
1122			
1075			ν(P–O)
1002			
980			
	978	976	
		960 sh	$\nu_{s,as}$(Mo=O_t)
955 sh			
938			
	925		
		918	
902		900	
	890		
		880	
870 sh			
	860	867	
825 sh			
	810		
	790		
776			
	730		
	720 sh	718	
ca. 700 sh			
ca. 635	ca. 645	647	
596			δ(O–P–O)
		ca. 585	
ca. 545 sh			
ca. 520			
	383	380	
	350		
		343	
	333		
	270	275 sh	
		257	
	240	240	ν_s(Mo–O)
		215 sh	
	183	178	
		158	
	85	76	
	55		
	40		

[a] Lyhamn, ref. 63.
[b] Lyhamn and Pettersson, ref. 64.

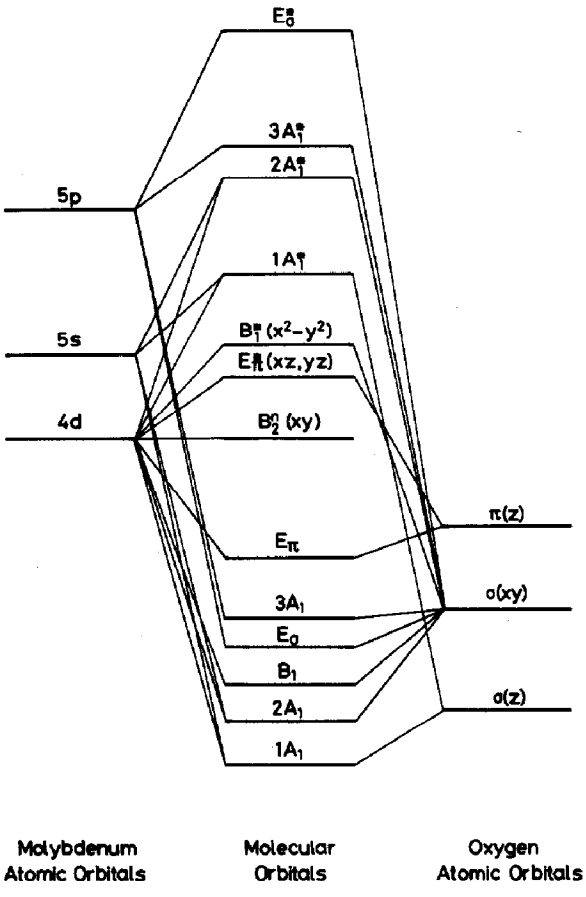

Fig. 8. Molecular orbital scheme for a MOL_5 complex, ref. 82.

structures. The classification of polymolybdates into structural types which depend on the number of terminal Mo=O bonds per MoO_6 unit can be related to the nature of the orbital which contains the added electron. Reducible molybdates of type a structure are analogous to $[MoOL_5]^-$ complexes. Here, taking $[MoOCl_5]^- \overset{+e^-}{\rightarrow} [MoOCl_5]^{2-}$ as an example, the first added electron resides in a non-bonding b_2 (d_{xy}) orbital in a MO scheme similar to that derived by Ballhausen and Gray [82] (see Fig. 8) for $[VOL_5]$ complexes of C_{4v} symmetry. The first added electron in a polymolybdate is weakly trapped on a molybdenum atom in a similar manner. The delocalisation of the electron is brought about by a combination of two effects. The first is a thermally activated hopping process between molybdenum atoms and the second involves a ground state delocalisation which is normally quite small. The intensity of the intervalence charge-transfer transition for reduced polymolybdates is dependent upon the degree of ground-state delocalisation. According to Hush [65] the energies of these transitions can be related to the

thermal hopping process by:

$$E_{op} = 4E_{th}$$

where E_{op} = energy of the intervalence charge-transfer transition,
E_{th} = activation energy for thermal hopping.

An increase in the ground-state delocalisation leads to a decrease in E_{th}. The electronic properties of reduced molybdates, tungstates and to a limited extent vanadates have been described elsewhere by Pope [4]. We describe below the electronic properties inferred from the e.s.r., electronic, and resonance Raman spectra of polymolybdates as a single class of compounds.

(i) Electronic spectra

Unreduced polymolybdates show charge-transfer transitions (oxygen to molybdenum) in the ultraviolet part of the spectrum. Solutions containing $[MoO_4]^{2-}$ give rise to spectra with an absorption maximum at ca. 47000 cm^{-1} which can be assigned to the Mo ← O charge-transfer transition [66]. The transitions observed for polymolybdates at 30000 to 48000 cm^{-1} are of a similar nature (see Jørgensen's optical electronegativities [67]). As the pH of a molybdate solution is lowered, the absorption maximum moves to longer wavelengths [68] and a second band appears between 30000 and 40000 cm^{-1} [66]. It is now well established that polymolybdates form on acidification of molybdate solutions [3,6] and that this absorption is due to the formation of Mo–O–Mo bridges [66].

Electronic spectra characteristic of reduced polymolybdates show bands in the visible and near-infrared regions. These are of two types: *d–d* bands for a Mo^{V} centre in a roughly C_{4v} site and inter-valence charge-transfer transitions (IVCT) between Mo^{V} and Mo^{VI} via an oxo-bridge. Depending on the nature of the reduced anion, the IVCT transitions are of moderate intensity (200–1000 M^{-1} cm^{-1}). The extinction coefficients also increase with the degree of reduction [69]. However, the intensities and positions of the Mo ← O bands are largely unaffected by reduction and only lose intensity slightly as reduction proceeds.

Molybdenum blues are modelled by substitution of V^{IV} for Mo^{VI} in Lindqvist–Aaronsson and Keggin molybdates. The degree of trapping of the valence electron is greater in the vanado-substituted molybdate than in the ordinary molybdenum blue [58] and these compounds are more stable with respect to re-oxidation [34,58]. On an electronic time-scale the valence electron appears to be trapped on a Mo^{V} site, even at room temperature and hence Mo^{V} *d–d* bands are observed along with the absorption maxima due to IVCT transitions.

The hexamolybdates possess only edge-shared MoO_6 octahedra. As a

consequence only one type of IVCT transition is expected. This is the so-called "intragroup" transition between MoO_6 octahedra sharing edges. By analogy with monomeric $[Mo^{V}OCl_5]^{2-}$ complexes, the Mo^{V} ion is at a site of approximately C_{4v} symmetry and should show d–d transitions from the $^2B_2$ ground state.

The spectrum of the brown one-electron-reduced $[Mo_6O_{19}]^{3-}$ anions shows bands at 20400, 11600 and ca. 9000 cm^{-1} which can be assigned to the $^2B_1 \leftarrow {}^2B_2$ and $^2E \leftarrow {}^2B_2$ transitions for Mo^{V} and to the intra-group IVCT transition, respectively [70,71]. The intensity of the IVCT transition at ca. 9000 cm^{-1} has been observed to be quite low (ca. 200 $M^{-1}\,cm^{-1}$) and this has been attributed to weak ground-state delocalisation of the valence electron. For the substituted molybdotungstate $[Mo^{V}W_5^{VI}O_{19}]^{3-}$, which is a one-electron blue, no band attributable to an IVCT transition is observed (presumably due to low intensity) and only red-shifted d–d bands for Mo^{V} are seen (Fig. 9) [22].

A series of substituted vanadium(V)–hexamolybdates has been prepared by Chauveau [72] and Labonnette and Ostrowetsky [73]. The latter have also reported the electronic spectra for complexes such as $[V_3^{IV}Mo_3^{VI}O_{19}H_6]^{2-}$, $[V_4^{IV}Mo_2^{VI}O_{19}H_7]^{3-}$ and $[V_2^{IV}Mo_4^{VI}O_{19}H_3]^{3-}$ [74] which contain V^{IV}, but no assignments were given (see Fig. 10).

V^{V} and V^{IV} substituted hexamolybdates have been studied by Buckley and Clark [34] who have reported spectra for both $[V^{V}Mo_5O_{19}]^{3-}$ and

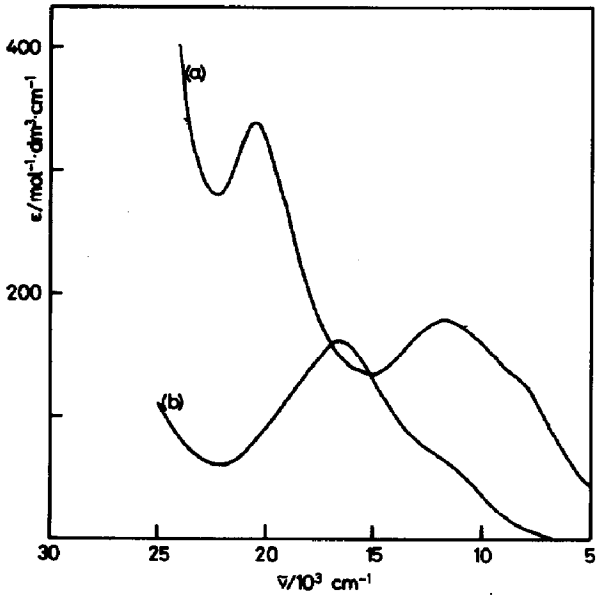

Fig. 9. Electronic spectra of one-electron reduced hexamolybdates. (a) $[Mo_6O_{19}]^{3-}$ in DMF solution and (b) $[W_5Mo^{V}O_{19}]^{3-}$ in DMF solution. Ref. 70.

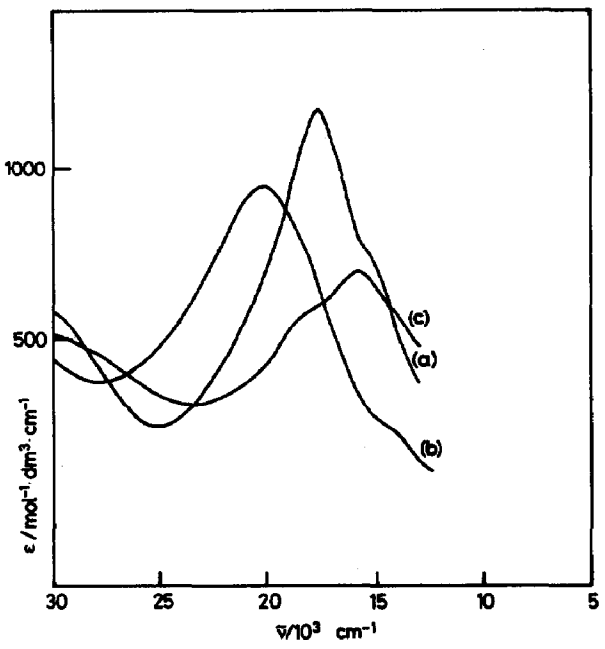

Fig. 10. Electronic spectra of vanadium(IV)-substituted hexamolybdates. (a) $[H_3V_2Mo_4O_{19}]^{3-}$ in aq. solution. (b) $[H_6V_3Mo_3O_{19}]^{2-}$ in aq. solution. (c) $[H_7V_4Mo_2O_{19}]^{3-}$ in aq. solution. (a), (b), and (c) ref. [74].

$[V^{IV}Mo_5O_{19}]^{4-}$; the latter compound is iso-electronic with a one-electron blue. Reported absorption spectra and some assignments for hexamolybdates are given in Table 8.

The electronic spectra of reduced dodecamolybdates are all similar to one another (see Fig. 11). Again, as with the structurally simpler, yet clearly related hexamolybdates, both IVCT and d–d (Mo^V) bands (or ligand-field bands of substituted ions) are observed. The two different edge- and corner-linkages between MoO_6 octahedra give rise to two different types of IVCT transition. Electronic transitions between MoO_6 octahedra sharing edges are known as "intra-group" and those between corner-shared octahedra are termed "extra-group".

Absorption bands in the near infrared part of the spectrum were attributed to intra-group and extra-group IVCT transitions by Fruchart et al. [69]. A survey of various reduced molybdates having the Keggin structure was carried out by these authors and it was found that the anions could be characterised by two or three absorption bands. Two of these are IVCT transitions and the third is assigned to the $^2E \leftarrow {}^2B_2$ transition for Mo^V. The intensity of the IVCT absorption bands increases on further reduction and also on changing from the α- to the β-isomer. Intra- and extra-group IVCT transitions were assigned to the bands at 7500–10200 and 10000–13000

TABLE 8

Absorption maxima (10^3 cm^{-1}) and assignments for the electronic spectra of one-electron reduced and vanadium(IV)-substituted hexamolybdates

Complex	Solvent	Absorption maxima/10^3 cm^{-1} (ϵ/M^{-1} cm^{-1})				Ref.
		Inter-valence charge-transfer		Mo^V or V^{IV} $d-d$ bands		
		Intra-group	Extra-group	$^2B_1 \leftarrow {}^2B_2$	$^2E \leftarrow {}^2B_2$	
				Mo^V		
$[Mo^V Mo_5^{VI} O_{19}]^{3-}$	DMF	ca. 9.0	–	20.4	11.6	70
$[Mo^V W_5^{VI} O_{19}]^{3-}$ [a]	DMF	–	–	16.7	11.3	70
				V^{IV}		
The following spectra [74] were not assigned.						
$[H_3 V_2^{IV} Mo_4^{VI} O_{19}]^{3-}$		–	–	17.7	15.0	74
$[H_8 V_3^{IV} Mo_3^{VI} O_{19}]$		–	–	20.2	14.5	74
$[H_6 V_3^{IV} Mo_3^{VI} O_{19}]^{2-}$		–	–	20.0	15.4	74
$[H_7 V_4^{IV} Mo_2^{VI} O_{19}]^{3-}$		–	–	18.6	15.8	74

[a] The $Mo^V \rightarrow W^{VI}$ IVCT is expected to be weak and blue shifted by ca. 5000 cm^{-1} [22]. Hence it is not observed.

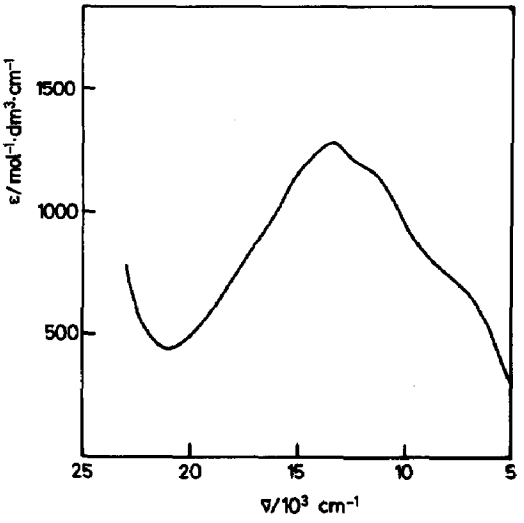

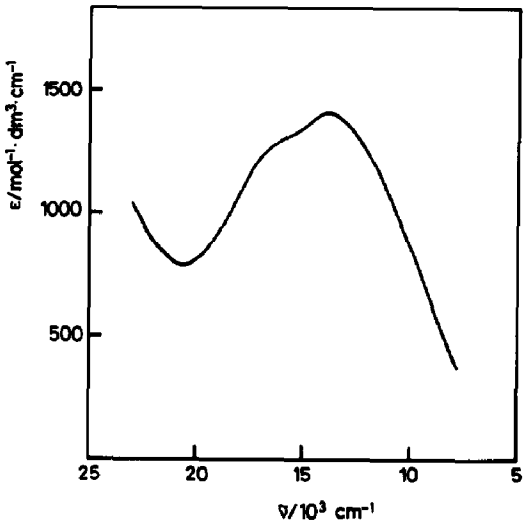

Fig. 11. Electronic spectrum of a one-electron reduced dodecamolybdate, α-$[SiMo_{12}O_{40}]^{5-}$, in DMF solution. Ref. 22.

Fig. 12. Electronic spectrum of a vanadium(IV)-substituted dodecamolybdate, $[PV^{IV}Mo_{11}O_{40}]^{6-}$, in aq. solution. Ref. 58.

cm^{-1}, respectively, by Fruchart et al. [69]. The $^2E \leftarrow {}^2B_2$ transition is at 18000 cm^{-1} and unaffected by either reduction of the anion or by a change from the α- to the β-form. The intra- and extra-group assignments were made on the observation of an intra-group IVCT transition at ca. 8000 cm^{-1} for both the α- and β-isomers of $[SiMo_3W_9O_{40}]^{5-}$. This assignment has recently been questioned by Sanchez et al. [22] in the light of more recent, more reliable data. Four $[X^{n+}Mo_{12}O_{40}]^{(8-n)-}$ (X = Si, P, Ge or As) anions were investigated by these authors. A band at 7000–8000 cm^{-1} for each reduced species was assigned to an IVCT. This assignment was supported by the absence of this absorption band for $[SiMo_{11}WO_{40}]^{5-}$.

The intra- and extra-group assignments of Fruchart et al. [69] to absorption maxima at ca. 8000 and 13000 cm^{-1} for heteropolymolybdates were made on the assumption that, at that time, three molybdenum atoms in $[SiMo_3W_9O_{40}]^{5-}$ belonged to the same Mo_3O_{13} group [75]. However, a more recent X-ray study has shown that the molybdenum atoms are in fact from different groups [76]. The intra-group IVCT transition can now be reassigned to the extra-group IVCT transition. The band at 13000 cm^{-1} has also been re-examined and shown to consist of the $^2E \leftarrow {}^2B_2$ and an IVCT transition [22]. Octahedra within a Mo_3O_{13} group in Keggin molybdates are linked in the same manner as those in $[Mo_6O_{19}]^{n-}$. Sanchez et al. [22] have pointed out that, as the inter-group IVCT transition occurs at ca. 8000 cm^{-1} for $[Mo_6O_{19}]^{3-}$, it is likely that both types of IVCT occur at similar

wavenumbers for dodecamolybdates (i.e. between 7000 and 9000 cm^{-1}).

A partially resolved band observed by the same authors at ca. 12000 cm^{-1} for dodecamolybdates has been tentatively assigned to a third IVCT transition. A band at ca. 18000 cm^{-1} (also observed by Fruchart et al. [69]) and a component of the 12000 cm^{-1} absorption maximum were assigned to Mo^{V} d–d transitions. The basis for this assignment is that the electronic interactions between two corner-shared octahedra give rise to an excited state which is involved in the IVCT. This state cannot be considered to be localised on one molybdenum ion, and two d_{xy} orbitals from two neighbouring Mo^{VI} ions interact to give rise to two excited bonding and antibonding levels. Two distinct IVCT transitions can thus be envisaged for the extra-group transition. One contributes to the 7000–8000 cm^{-1} band (along with the intra-group IVCT transition) and the second can explain a shoulder seen at 11500 cm^{-1}. An estimate of the electronic interactions within different molybdate structures can be obtained by comparing the intensities of the IVCT bands. Interactions between corner-shared MoO_6 units are greater than those between edge-shared octahedra (compare the intensities of the respective transitions for $[Mo_6O_{19}]^{3-}$ and $[SiMo_{12}O_{40}]^{5-}$). The weak intensity of the intra-group IVCT transition accounts for its non-appearance in dodecamolybdate spectra, where it is probably obscured by the more intense extragroup IVCT transition. Thus there is more extensive ground-state delocalisation in Keggin molybdates than in Lindqvist–Aaronsson structures.

The spectra described above are for non-protonated dodecamolybdates mainly in solution. The degree of protonation of molybdates often has a marked effect on their absorption spectra. This aspect has been discussed by Massart [77].

Tanaka et al. [78] have recently carried out a spectro-electrochemical investigation of the reduction of dodecaphosphomolybdic acid in aqueous solution. They demonstrated that the first two two-electron reductions are reversible but that the six-electron reduction product changes quickly to other heteropolyanions.

Photochemical reduction of dodecamolybdates with the Keggin structure has been interpreted spectroscopically by Back and So [79] and Buckley and Clark [56], and their results are described in a later section.

Vanadium-substituted Keggin dodecamolybdates such as $[PVMo_{11}O_{40}]^{4-}$ and $[PV_2Mo_{10}O_{40}]^{5-}$ and $[PV_3Mo_9O_{40}]^{6-}$, which are isoelectronic with unreduced heteropolyanions, show a characteristic absorption at 32200 cm^{-1} ($\epsilon = 17000$–$18000\ M^{-1}\,cm^{-1}$) [61].

Heteropolymolybdates substituted with V^{IV}, i.e. iso-electronic with the reduced blues, are characterised by one or two intense absorption bands in the visible region assigned to IVCT transitions ($Mo^{VI} \leftarrow V^{IV}$). Vanadium is

TABLE 9

Absorption maxima (10^3 cm^{-1}) and assignments for the electronic spectra of one-electron reduced and vanadium(IV)-substituted dodecamolybdates and one-, two-, four-, and six-electron reduced octadecamolybdates

Complex	Solvent	Absorption maxima/10^3 cm^{-1} (ϵ/M^{-1} cm^{-1})					Ref.
		Inter-valence charge-transfer		Mo^V or V^{IV} $d-d$ bands			
		Intra-group + Extra-group I	Extra-group II	$^2E \leftarrow {}^2B_2$		$^2B_1 \leftarrow {}^2B_2$	
					Mo^V		
α-$[SiMo_{12}O_{40}]^{5-}$	DMF	–		13.3		18.5(sh)	69
		7.0(sh)	11.5(sh)		13.3	18.5(sh)	22
α-$[SiMo_{12}O_{40}]^{5-}$		7.5(sh)		10.3		–	69
α-$[PMo_{12}O_{40}]^{4-}$		6.4, 8.6	11.6		13.5	18.5	22
	1:1, H_2O: Dioxan	–		12.8		–	78
$[GeMo_{12}O_{40}]^{5-}$		7.3	11.6		13.7	–	22
$[AsMo_{12}O_{40}]^{4-}$		–	11.9		13.05	–	22
α-$[HP_2Mo_{18}O_{62}]^{6-}$				13.3		16.7	81
α-$[H_2P_2Mo_{18}O_{62}]^{6-}$		9.0	13.2	not assigned			80
α-$[H_4P_2Mo_{18}O_{62}]^{6-}$		11.2	14.8				80
α-$[H_6P_2Mo_{18}O_{62}]^{6-}$		14.5	16.7				80

The assignments of the spectra taken from ref. 69 and 81 have been corrected in the table (see Section D(i))

Vanadium-substituted dodecamolybdates		IVCT: $V^{IV} \rightarrow Mo^{VI}$	V^{IV} $d-d$		Ref.
$[PV^{V}Mo_{11}^{VI}O_{40}]^{4-}$ [a]	Aq.	–	–		58
$[PV^{IV}Mo_{11}^{VI}O_{40}]^{5-}$	Aq.	15.2	–	–	58
$[SiV^{IV}Mo_{11}^{IV}O_{40}]^{6-}$	Aq.	15.7	–	–	58

[a] O $\leftarrow$ Mo charge-transfer transition at 32.2×10^3 cm^{-1}.

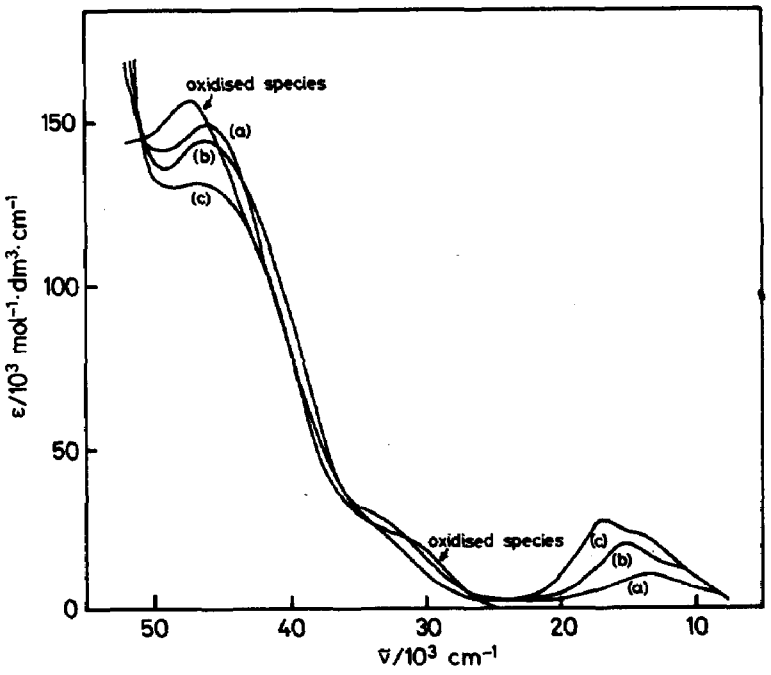

Fig. 13. Electronic spectra of reduced octadecamolybdates. (a) α-$[H_2P_2Mo_{18}O_{62}]^{6-}$ in aq. solution. (b) α-$[H_4P_2Mo_{18}O_{62}]^{6-}$ in aq. solution. (c) α-$[H_6P_2Mo_{18}O_{62}]^{6-}$ in aq. solution. Ref. 80.

more easily reduced than molybdenum [58] and the extent of localisation of the valence electron, in a one-electron blue, has been calculated, using Hush's formula [65], by Altenau et al. [58] for $[PVMo_{11}O_{40}]^{5-}$. The electron was found to be 96.6% localised using data derived from the wavenumber of the IVCT transition at 15200 cm^{-1}. Spectra and band wavenumbers and assignments are shown in Fig. 12 and Table 9, respectively.

The two-, four- and six-electron blues ($[H_2P_2Mo_{18}O_{62}]^{6-}$, $[H_4P_2Mo_{18}O_{62}]^{6-}$, and $[H_6P_2Mo_{18}O_{62}]^{6-}$) which have the Dawson α-structure, show broad absorption bands in the 10000–16000 cm^{-1} region of the spectrum; these bands are gradually blue-shifted with both reduction and protonation [80] (see Fig. 13). The intensities of these bands are proportional to the degree of reduction ($\epsilon = 5000\ M^{-1}\ cm^{-1}/Mo^{V}$). Mo ← O charge-transfer transitions also occur at 30000–40000 cm^{-1} and are largely unaffected by reduction.

The formerly unknown one-electron reduction of $[P_2Mo_{18}O_{62}]^{6-}$ has been observed by Papaconstantinou and Hoffman [81]. The one-electron blue was prepared by pulse radiolysis generation of radicals capable of transferring a single electron only. The reactions occurring in solution in methanol, ethanol and 2-propanol were of the following type:

$$[P_2Mo_{18}O_{62}]^{6-} + \dot{R}COH \rightarrow [HP_2Mo_{18}O_{62}]^{6-} + RC{=}O$$

$(R = CH_3, C_2H_5, \text{or } C_3H_7)$.

The one-electron blue is characterised by two absorption bands at 13300 and ca. 16700 cm^{-1}, assigned to an IVCT transition and a Mo^V d–d transition, respectively. The absorption band at 13000 cm^{-1} was thought to be an intra-group IVCT, but it is more likely that it is an extra-group IVCT transition with the former being in the near infrared. Unfortunately measurements were not made at wavelengths longer than 800 nm because of "strong absorptions", presumably due to the missing IVCT transition.

Back and So [79] have observed bands at ca. 18000, 13300 and 8600 cm^{-1} for $[P_2Mo_{18}O_{62}]^{7-}$ in a PVA film and these are discussed later.

(ii) Electron spin resonance spectra

The e.s.r. spectrum for a Mo^V ion in an axial ligand field can be described by the following spin-Hamiltonian:

$$H = g_{\parallel}\beta H_z S_z + g_{\perp}\beta(H_x S_x + H_y S_y) + A_{\parallel} S_z I_z + A_{\perp}(S_x I_x + S_y I_y)$$

Here the main axis for both the axially symmetric g and A tensors is taken as the direction of the short M=O bond, i.e. this is the z-axis [22]. Using the LCAO-MO method followed by Ballhausen and Gray [82] for MOL_5 type complexes with d^1 electronic configurations and C_{4v} symmetry, one can obtain the ligand field orbitals for Mo^V described below (see Fig. 8). These are the orbitals involved in π-bonding with the ligands.

$$\left.\begin{aligned} |B_2\rangle &= \beta_2|d_{xy}\rangle - \beta_2'|\phi_{B_2}\rangle \\ |B_1\rangle &= \beta_1|d_{x^2-y^2}\rangle - \beta_1'|\phi_{B_1}\rangle \\ |E\rangle &= \epsilon|d_{xz}, d_{yz}\rangle - \epsilon'|\phi_{E_x,E_y}\rangle \end{aligned}\right\} \text{approximate energy ordering}$$

The ligand orbitals, ϕ, are group orbitals of the appropriate symmetry. The e.s.r. parameters, g and A, can then be described as follows [83]:

$$g_{\parallel} - 2.0023 = -\left[\frac{2(2\lambda_M\beta_2\beta_1 - \lambda_L\beta_2'\beta_1')}{\Delta E(B_1 \leftarrow B_2)}\right](2\beta_2\beta_1 - 2\beta_1\beta_2' S_{B_2} - 2\beta_2\beta_1' S_{B_1} - \beta_1'\beta_2')$$

and

$$g_{\perp} - 2.0023 = -\left[\frac{2\lambda_M\beta_2\epsilon}{\Delta E(E \leftarrow B_2)}\right](\beta_2\epsilon - \beta_2\epsilon' S_E - \epsilon\beta_2' S_{B_2})$$

The quantity ΔE is the energy of the transition given in parentheses and the parameters S_{B_1}, S_{B_2} and S_E are the overlap integrals for the appropriate orbitals. λ_L and λ_M are the spin–orbit coupling constants for the ligands and the metal ion, respectively.

The hyperfine tensor components $A_{\|}$ and $A_{\perp}$ can be described thus:

$$-\frac{A_{\|}}{P} = K\beta_2^2 + \tfrac{4}{7}\beta_2^2 + 2.0023 - g_{\|} + \tfrac{3}{7}(2.0023 - g_{\perp})$$
$$+\left[\frac{6}{7}\frac{\lambda_M\beta_2\epsilon}{\Delta E(E \leftarrow B_2)}\left(\beta_2\epsilon' S_E + \epsilon\beta_2' S_{B_2}\right)\right]$$
$$+\left[\frac{2(2\lambda_M\beta_2\beta_1 - \lambda_L\beta_2'\beta_1')}{\Delta E(B_1 \leftarrow B_2)}\right]\left(2\beta_2\beta_1' S_{B_1} + 2\beta_1\beta_2' S_{B_2} + \beta_1'\beta_2'\right)$$

and

$$\frac{A_{\perp}}{P} = K\beta_2^2 - \tfrac{2}{7}\beta_2^2 + \tfrac{11}{14}(2.0023 - g) + \frac{11}{7}\frac{\lambda_M\beta_2\epsilon}{\Delta E(E \leftarrow B_2)}\left(\beta_2\epsilon' S_E + \epsilon\beta_2' S_{B_2}\right)$$

where $P = 2\beta_0\gamma_N\beta_N\langle r^{-3}\rangle$ and K is the Fermi isotropic interaction constant. Ché et al. [70] have solved the above equations for the e.s.r. parameters for Mo^V to obtain values for β_1, β_2, ϵ, and K.

β_1', β_2', and E' can be related to the corresponding coefficients by normalisation:

$$\beta_2^2 + (\beta_2')^2 - 2\beta_2\beta_2' S_{B_2} = 1$$

Approximate values for β_2 can be obtained from the expressions describing $A_{\|}$ and $A_{\perp}$:

$$\beta_2^2 = \tfrac{7}{6}\left[\frac{(A_{\perp} - A_{\|})}{P}\right] - \tfrac{7}{6}(2.0023 - g_{\|}) + \tfrac{5}{12}(2.0023 - g_{\perp})$$

The overlap terms, S, are not considered and the equation is not affected by the nature of the optical transitions. This is advantageous as the electronic spectra of reduced molybdates are often dominated by intense IVCT transitions (see previous section). Values obtained for β_2 can be used to give an indication of the extent of ground-state delocalisation of the valence electrons in molybdenum blues.

The simplest isopolymolybdate yields a one-electron "blue", $[Mo_6O_{19}]^{3-}$, which is brown! Ché et al. [70] and Sanchez et al. [22] have investigated the e.s.r. spectrum of this species using the above approach to interpret their results.

Spectra were recorded at both low- and room-temperature. At 77 K a frozen dimethylformamide solution spectrum was recorded which was characteristic of a Mo^V ion in an axial ligand-field with hyperfine splitting due to the interaction of the unpaired electron with the molybdenum isotopes of nuclear spin $I = 5/2$. As the temperature is raised the signal broadens and at 300 K the spectrum consists of a single line without hyperfine splitting.

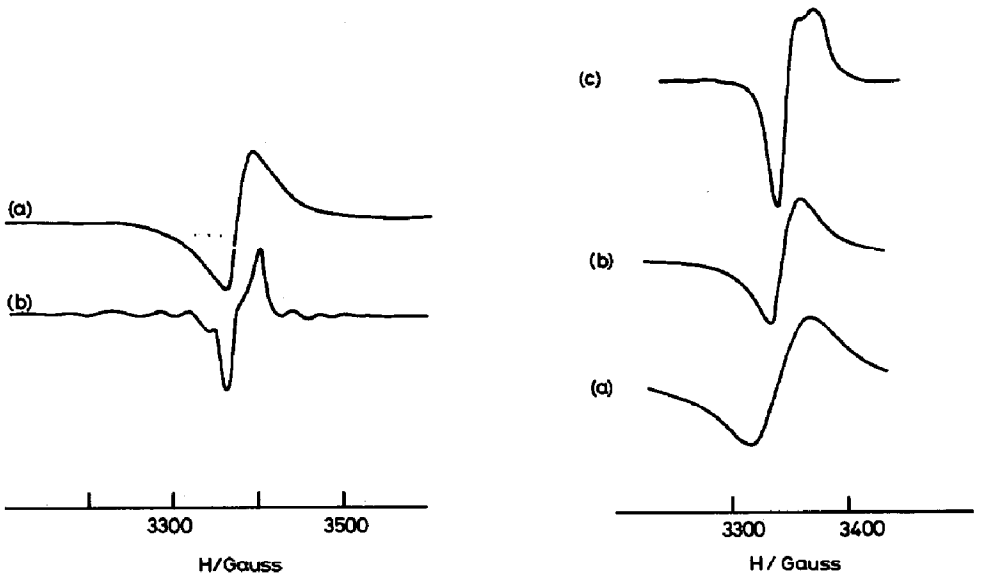

Fig. 14. E.s.r. spectra of $[Mo_6O_{19}]^{3-}$. (a) DMF solution at room-temperature. (b) Frozen DMF solution at 10 K. (a) and (b) ref. 22.

Fig. 15. E.s.r. spectra of $[GeMo_{12}O_{40}]^{5-}$ in DMF solution at (a) 140 K, (b) 70 K, and (c) 10 K. Ref. 22.

From the axial spectrum the following e.s.r. parameters were obtained: $g_\perp = 1.930$, $A_\perp = 34.5$ G; $g_\parallel = 1.919$, $A_\parallel = 80.5$ G. The frozen solution spectrum showed good resolution up to ca. 110 K [22] whereupon it broadens and the hyperfine splitting disappears at temperatures above 117 K. The line broadening was found to increase with temperature and at ca. 200 K a Lorentzian signal was seen. Observed e.s.r. spectra are shown in Fig. 14 and e.s.r. parameters are given in Table 10.

The above results are consistent with a Mo^V centre in axial, C_{4v}, symmetry at low temperatures; this is effectively the site of the odd electron (cf. electronic spectra in which the time scale of the measurement is such that the unpaired electron appears trapped even at room temperature). The disappearance of the hyperfine splitting at temperatures above ca. 110 K also shows that thermal delocalisation of the electron occurs via a hopping process. This process, Mo^V–O–$Mo^{VI} \rightarrow Mo^{VI}$–O–$Mo^V$, was deduced by Ché et al. [70] to have a frequency of ca. 5×10^7 Hz.

The easy observation of the spectrum at room-temperature also suggested that the single unpaired electron resides in an orbitally non-degenerate ground-state, i.e. a $b_2(d_{xy})$ orbital as suggested by Pope [7]. A value of 0.92 for the parameter β_2 (the molecular orbital coefficient associated with equatorial π-bonding [70]) was obtained.

TABLE 10

Isotropic and anisotropic e.s.r. parameters for one-electron reduced hexa- and dodecamolybdates and vanadium(IV)-substituted dodecamolybdates

(a) Isotropic parameters for vanadium(IV)-substituted molybdates at 298 K [a]

	$\langle g \rangle$	$\langle \alpha \rangle$ (10^{-4} cm^{-1})
$[PVMo_{11}O_{40}]^{5-}$	1.964	83.4
$[SiVMo_{11}O_{40}]^{6-}$	1.965	83.3

(b) Anisotropic parameters for one-electron reduced dodecamolybdates [b]

	$g(g_z)$	$g(g_x,g_y)$	$A_{\parallel}$	$A_{\perp}$ (10^{-4} cm^{-1})
$[Mo_6O_{19}]^{3-}$	1.919	1.930	80.5	34.5 [c]
	1.916	1.930	80.5	33.5
α-$[SiMo_{12}O_{40}]^{5-}$	1.931	1.944	65.5	32.0
$[GeMo_{12}O_{40}]^{5-}$	1.935	1.951	68.5	33.6
α-$[PMo_{12}O_{40}]^{4-}$	1.938	1.949	60.7	27.2
$[AsMo_{12}O_{40}]^{4-}$	1.935	1.948	64.4	28.2

[a] Altenau et al. ref. 58.

[b] Sanchez et al. ref. 22, except for the first entry which is from Ché et al. [c].

[c] Ché et al. ref. 70.

E.s.r. spectra for a number of one-electron reduced dodecamolybdates have been reported and the values for their e.s.r. parameters, together with those for $[Mo_6O_{19}]^{3-}$, are given in Table 10. The spectra (see Fig. 15) are all indicative of the unpaired electron being trapped on a single molybdenum atom at sufficiently low temperatures [22,83,84]. As for hexamolybdates, thermal delocalisation of the valence electron occurs as the temperature is raised.

The extent of ground-state delocalisation, as measured by the parameter β_2, differs from Lindqvist to Keggin molybdates. The e.s.r. data for $[PMo_{12}O_{40}]^{4-}$ show that the unpaired electron is more delocalised than in $[Mo_6O_{19}]^{3-}$, a deduction also made from their electronic spectra. A measure of the extent of delocalisation can be obtained by comparing values of β_2. For $[PMo_{12}O_{40}]^{4-}$ β_2 has a value of 0.79 whereas $[Mo_6O_{19}]^{3-}$ has a β_2 value of 0.92, indicating more extensive ground-state delocalisation in the former.

Sanchez et al. [22] and Launay et al. [83] have used the results obtained by Ché et al. [70] to show that the ground-state delocalisation for $[Mo_6O_{19}]^{3-}$ is restricted to the ligand oxygen atoms and does not involve the neighbouring molybdenum atoms. On the other hand the delocalisation of the valence electron for $[PMo_{12}O_{40}]^{4-}$ does involve the neighbouring metal atoms and is consequently more pronounced. The differences between the ground-state delocalisation for hexa- and dodecamolybdates are demonstrated quite clearly by the disappearance of hyperfine splitting at 50 K for $[PMo_{12}O_{40}]^{4-}$ but at ca. 110–120 K for $[Mo_6O_{19}]^{3-}$.

E.s.r. spectra for $[(C_4H_9)_4N]_4[PMo_{12}O_{40}]$ as a solid solution in $[(C_4H_9)_4N]_4[SiW_{12}O_{40}]$ were at first reported to be completely isotropic at low temperatures [85,86], i.e. from 50 down to 6 K. Six hyperfine splitting lines were also observed in the spectrum. This presented Prados et al. [85,86] with a situation which was difficult to interpret. The isotropic central line suggested a rapid exchange of electrons but, at the same time, the presence of hyperfine splitting indicated a localised valence with a Mo^V centre. The later work of Sanchez et al. [22] and Launay et al. [83] on frozen dimethylformamide solutions demonstrated that, from the shape of the central line, the crystal field is slightly rhombic, as deduced previously by Zaitov [87], and that the unpaired electron is actually trapped at low-temperatures. Similar results have been found by Rabette et al. [84] for dodecasilicomolybdic acid. Dodecamolybdate e.s.r. spectra are shown in Fig. 15. E.s.r. spectra for $H_3[PMo_{12}O_{40}]$ in various states of reduction have been reported by Eguchi et al. [88], Mizuno et al. [55], and Otake and Otaki [89]. The heteropolyacid was reduced with H_2 and the reduction mechanism was followed using e.s.r. and infrared spectroscopy. It was found by all of the authors that the intensity of the e.s.r. signal, due to Mo^V formation, was proportional to the degree of reduction. A rise in temperature up to 573 K also caused an increase in the signal intensity.

Vanadium(IV) substituted dodecamolybdates have also been investigated as models for heteropoly blues. The work of Otake et al. [90] on $H_5[PV^{IV}Mo_{11}O_{40}]$ in aqueous solutions now seems to be invalid as it is thought that the conditions used for reduction bring about decomposition of the molybdate [58]. Solutions of $[PV^VMo_{11}O_{40}]^{4-}$ were treated with organic compounds or H_2 and the spectra of the subsequent reduction products were recorded.

Maksimovskaya et al. [91] have observed e.s.r. spectra for vanadium-substituted heteropoly acids such as $[PVMo_{11}O_{40}]^{5-}$ and $[PV_2Mo_{10}O_{40}]^{6-}$ which were produced by reducing the corresponding acids with hydrazine hydrate. It was found that V^V is reduced in preference to Mo^{VI} and that the subsequent e.s.r. spectra could be interpreted as arising from the interaction of the unpaired electron with the ^{51}V nucleus ($I = 7/2$), thus giving rise to an eight-line hyperfine splitting. The spectra were measured as frozen solutions and show axial anisotropy. The solution spectrum was also identical to that of polycrystalline $K_3H[PVMo_{11}O_{40}] \cdot 5H_2O$ after mild reduction. During the solution studies it was also found that a decrease in pH gave rise to the formation of $[VO(H_2O)_5]^{2+}$. More vigorous reduction was found to reduce Mo^{VI} to Mo^V but this product was not detectable by e.s.r. spectroscopy. As for the reduction of $[PV_2Mo_{10}O_{40}]^{4-}$, an initial fifteen-line spectrum was interpreted as being due to the sum of the spectra of $[PVMo_{11}O_{40}]^{5-}$ and $[PV_2Mo_{10}O_{40}]^{5-}$.

Altenau et al. [58] have recorded the e.s.r. spectra of $[X^{n+}V^{IV}Mo_{11}O_{40}]^{(10-n)-}$ (X = P or Si). The spectra indicated that the electron is, again, localised on a V^{IV} site rather than a Mo^{V} one.

The difference between the extent of ground-state delocalisation for hexa- and dodecamolybdates can be rationalised using symmetry and by comparing the two structures. Using simple symmetry arguments, the possibility of $Mo(d_{xy})$–$O(p_{\pi})$–$Mo(d_{xy})$ overlap between corner-shared octahedra ($[XMo_{12}O_{40}]^{n-}$ structure) is greater than that between edge-shared MoO_6 units common to both types.

(iii) Resonance Raman spectra

Resonance enhancement of Raman scattering occurs when the wavelength of the exciting radiation coincides with that of a dipole-allowed electronic transition of the molecules under investigation. The Raman band associated with the vibration responsible for the vibronic structure of such an electronic transition is often greatly enhanced [60,92]. Excitation within the contour of the IVCT electronic transition of reduced polymolybdates may reveal, via the resonance Raman spectrum, the extent of localisation or delocalisation of the valence electron in the molybdate structure. The IVCT transitions of reduced polymolybdates occur in the red and near infrared regions (see section C(i)) and one faces an immediate problem—a lack of readily available laser lines of long wavelength to probe the IVCT.

To date the only resonance Raman spectroscopic investigations are those of Kasprzak [49] and Buckley and Clark [34,56] concerning both hexa- and dodecamolybdates. The former authors describe a spectrum which they attribute to the resonance Raman effect for dodecamolybdates. Excitation at a wavelength of 514.5 nm gave rise to a spectrum in which all of the vibrational modes were reported to have been enhanced. It was also described how exciting radiation of longer wavelength (i.e. 647.1 nm) was strongly absorbed by the deep blue compounds. This feature was also observed by Buckley and Clark [56], who found that dimethylformamide solutions of $[SiMo_{12}O_{40}]^{4-}$, reduced by ultraviolet radiation, absorbed laser radiation of wavelength 647.1 and 676.4 nm. The reported enhancement of all of the vibrational modes [49] is a little peculiar in that they cannot all be associated with the same electronic transition. Also, the exciting laser radiation of wavelength 514.5 nm (19435 cm^{-1}) is removed from the wavenumber of the closest IVCT transition which, for dodecamolybdates, occurs at 12000–15000 cm^{-1}. It is, however, close to a *d–d* band at 18000 cm^{-1}. As a consequence of the above, resonance enhancement would not be expected in any of the vibrational modes. It seems, therefore, that Kasprzak et al. [49] have observed a straightforward Raman spectrum of $[SiMo_{12}O_{40}]^{5-}$.

On the other hand, Buckley and Clark [34] have observed resonance enhancement of the δ(Mo–O–Mo) mode for the vanado-substituted hexamolybdate $[V^{IV}Mo_5O_{19}]^{4-}$. A similar effect was also observed for $Mo_4O_{10}(OH)_2$, a two-electron, neutral blue. The enhancement of δ(Mo–O–Mo) is not great and overtones associated with it were not observed (see Fig. 16). According to resonance Raman theory and various models for mixed-valence complexes [36,92], the enhancement of a single mode in the absence of an overtone progression indicates that the resonant transition occurs between delocalised orbitals, and thus that no single coordinate suffers any substantial geometric change on excitation of the complex to the resonant excited state. This is not quite the expected situation as vanadomolybdates are thought to show the properties of localised systems where the electron is localised largely on the vanadium atom. The situation is not yet clear and more work is in progress.

Attempts have also been made by Buckley and Clark [56] to record resonance Raman spectra of one- and two-electron reduced dodecamolybdates such as $[SiMo_{12}O_{40}]^{n-}$ and $[PMo_{12}O_{40}]^{n-}$. The α- and β-isomers of $[SiMo_{12}O_{40}]^{4-}$ were doped into PVA film and then irradiated with ultraviolet light (see section E). These molybdates were also irradiated when in solution in dimethylformamide. Attempts to record spectra were largely unsuccessful due to absorption of the exciting radiation at long wavelengths (≥ 650 nm) and decomposition of both the sample and the PVA film in the beam.

The usual classification scheme for mixed-valence compounds [5] can be used to describe the extent of electron delocalisation in one-electron reduced polymolybdates. In this scheme anions such as $[PMo^{V}Mo^{VI}_{11}O_{40}]^{4-}$ show quite weak valence trapping and belong to class II with quite extensive ground-state delocalisation. The vanadium(IV)-substituted complexes can be placed somewhere between class I, where the valence-electron is strongly trapped, and class II.

Clearly, the distinctions are blurred for these compounds as they all show different degrees of ground-state delocalisation, both within a class ($[PV^{IV}Mo^{VI}_{11}O_{40}]^{5-}$ and $[PMo^{V}Mo^{VI}_{11}O_{40}]^{4-}$) and between two different types ($[Mo^{V}Mo^{VI}_{5}O_{19}]^{3-}$ and $[PMo^{V}Mo^{VI}_{11}O_{40}]^{4-}$).

E. PHOTOCHEMICAL REDUCTION OF POLYMOLYBDATES

The one-electron reduction of heptamolybdate $[Mo_7O_{24}]^{6-}$ (a type b structure with *cis*-dioxo groups) can be effected by irradiating aqueous solutions or single crystals of alkylammonium salts with ultraviolet light [11,12,93–101]. Hepta- and octamolybdates $[Mo_8O_{28}]^{8-}$ can also be reduced to one-electron blues by irradiation with γ- and X-rays [13,102]. The mecha-

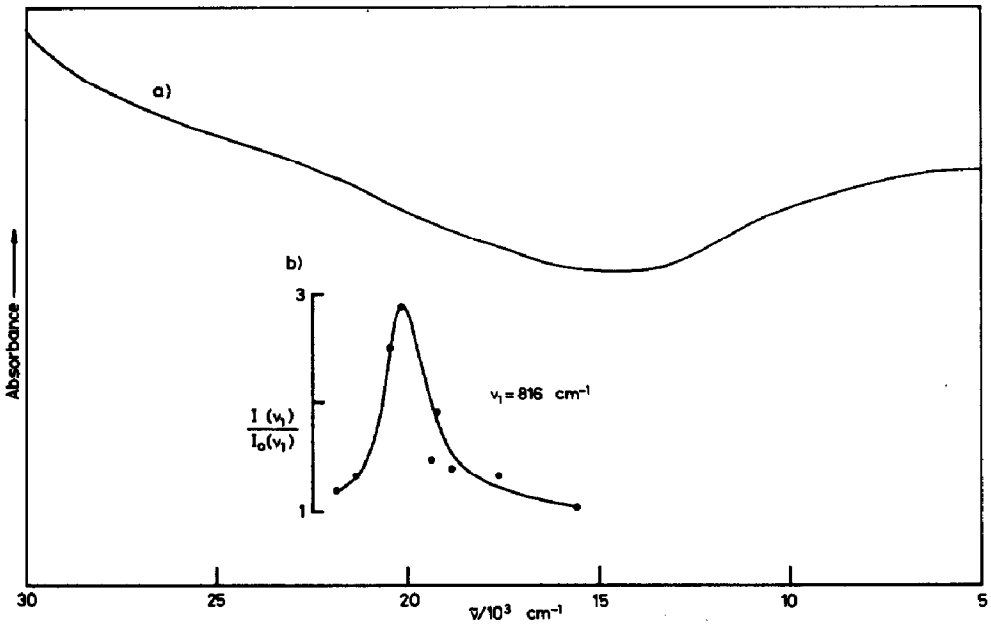

Fig. 16. (a) Electronic spectrum (transmission, Nujol mull) and excitation profile of the $\nu_1 = (816\ cm^{-1})$ band in the resonance Raman spectrum of $Mo_4O_{16}(OH)_2$, at ca. 80 K. Refs. 34 and 56.

nism of ultraviolet photoreduction has been investigated by Yamase et al. [11,93–100] using e.s.r. and electronic spectroscopy. Their proposed mechanism involves the formation of a charge-transfer complex between heptamolybdate and either the solvent or the alkylammonium cation [12,93–98].

Photoirradiation of aqueous heptamolybdate solutions at wavelengths of ca. 330 nm causes the photo-excitation of an oxygen-to-metal charge-transfer along a terminal Mo=O bond. This in turn induces the formation of a charge-transfer complex between heptamolybdate and the counterion with subsequent oxidation of H_2O to $\dot{O}H$ and reduction of Mo^{VI} to Mo^{V}. The charge-transfer complex is produced by a photon-induced proton transfer from the alkylammonium cation to a bridging (Mo–O_b–Mo) oxygen atom. The photoreaction scheme which occurs at MoO_6 sites is shown in Fig. 17. A competing reaction also occurs involving the oxidation of the alkylammonium cation (eqn. iii). However, the quantum yields of the products for this reaction have been shown to be small compared to those of Mo^{V} and $\dot{O}H$ [12]. Solutions containing acetic acid and acetylene have also been shown by Yamase et al. [12,98] to produce quantities of propylene and CO_2 and acetaldehyde, respectively (see Fig. 17). These reactions are, however, major competitors with the $\dot{O}H$-forming reaction.

Similar mechanisms have been proposed for the photoreduction of single crystals of isopropylammonium heptamolybdate by the same authors. These

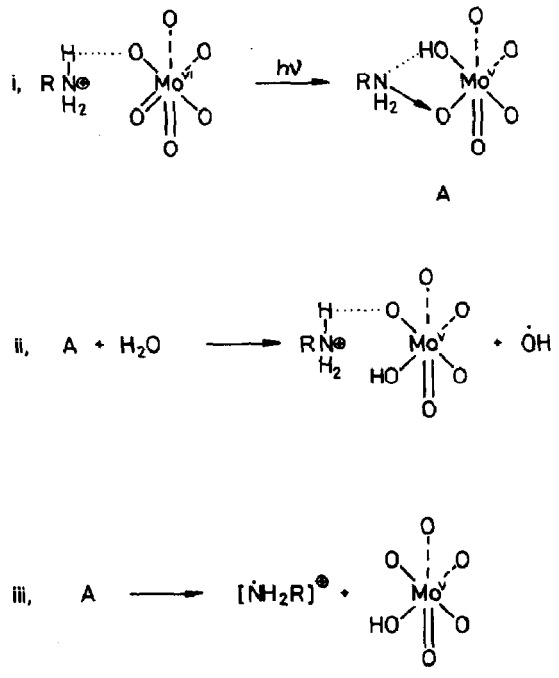

R=C_3H_7 ; $[RNH_3]^{\oplus}$ can be replaced by CH_3COOH.

Fig. 17. Reaction scheme for the photochemical reduction of $[Mo_7O_{24}]^{6-}$ in the presence of either alkylammonium cations, CH_3COOH, or C_2H_2.

effects have been investigated because of their use as models for the photogeneration of electron-hole pairs in n-type oxide semiconductors [12].

Similar studies have also been carried out in order to develop a solar-energy storage system based on water photolysis [99–101]. This type of photoreaction produces H_2 at the cathode of a photogalvanic cell when irradiated with ultraviolet light. Dye-sensitised photoreactions enable light of longer wavelength (i.e. visible light) to be used by providing a medium which absorbs light in the appropriate spectral region [101].

Back and So [79] and Buckley and Clark [56] have investigated ultraviolet-irradiated PVA films containing dodeca- and octadecamolybdates such as $[PMo_{12}O_{40}]^{3-}$ [56,79] and $[P_2Mo_{18}O_{62}]^{6-}$ [79]. Both working groups found that prolonged irradiation at wavelengths less than 350 nm, for periods of up to 24 hours, gave initially a one-electron blue with increasing amounts of the two-electron species (see Fig. 18). $[P_2Mo_{18}O_{62}]^{6-}$ was also found to show similar behaviour [79]. The use of PVA films provides a medium in which the photochemically reduced molybdate is stabilised (by a mechanism similar to that described above) and the blue colouration of the film persists for periods of up to a year.

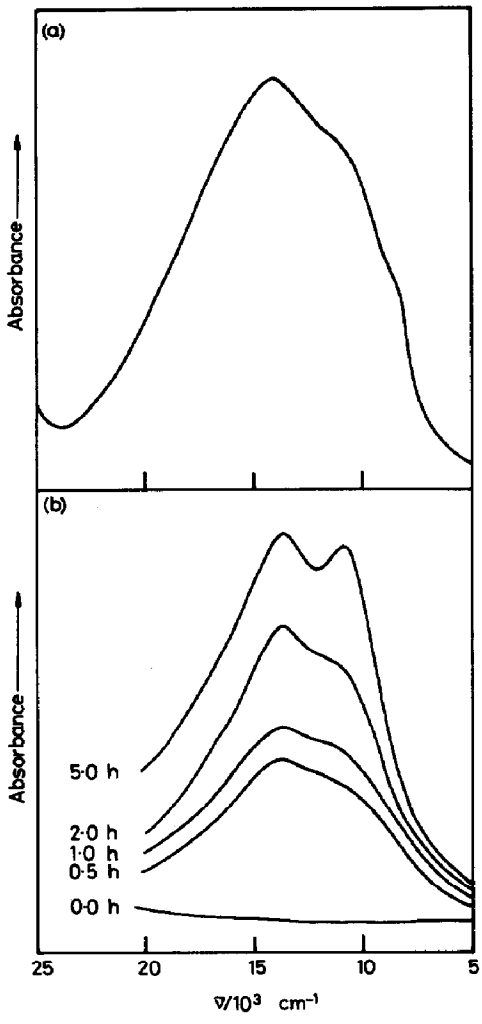

Fig. 18. Electronic spectra of U.V. irradiated $[SiMo_{12}O_{40}]^{4-}$. (a) DMF solution (10^{-3} M) after irradiation for 10 hours. (b) α-$[(CH_3)_2NH_2]_4[SiMo_{12}O_{40}]$ doped into a polyvinyl alcohol (PVA) film (5 cm^3 0.01 M soln. +1 g PVA) and irradiated for various periods of time. Ref. 56.

The ultraviolet irradiation of dimethylammonium salts of the α- and β-isomers of $[SiMo_{12}O_{40}]^{4-}$, as both solids and dimethylformamide solutions results in the formation of one- and two-electron blues. These processes were monitored using electronic spectroscopy by Buckley and Clark [56] and the spectra are shown in Fig. 18. It was also found, as expected [19], that the β-isomer is the more easily reduced. Photoreduction of the tetrabutylammonium salts was found not to proceed and it was assumed that, as this cation is a quaternary ammonium ion, a charge-transfer complex is not formed between molybdate and counterion.

F. CONCLUDING REMARKS

The preceding sections, although not forming an exhaustive review, have, we feel, covered the major topics concerning the spectroscopic properties which relate to the structural and electronic characteristics of polymolybdates.

It is clear that much work remains to be done in both fields. This is needed to resolve completely discrepancies in, for example, areas such as that of assigning the vibrational spectra of dodecamolybdates. Resonance Raman spectroscopy on reduced molybdates may also be fruitful in elucidating further the mixed-valence nature of these compounds. To that end work is in progress in this laboratory.

ADDENDUM

Since this review was written it has come to our attention that an excellent review of molybdate chemistry has been published by Pope [103]. Although we discuss structural types, and some of the electronic properties of molybdenum blues in a similar manner, we differ by describing the vibrational spectroscopy in detail along with some aspects of the photochemistry of polymolybdates. The discussion given by Pope of the electronic spectra of reduced molybdates drops the intra- and extra-group assignments for IVCT transitions as proposed by Fruchart et al. [69] and instead uses an alternative description. For 12- and 18-molybdates, the approximation to C_{4v} symmetry for the Mo^{V} site is no longer valid as opposed to the situation for $[Mo_6O_{19}]^{3-}$. The symmetry is better described as rhombic (ca. C_s), even though this assumption is not borne out by previous e.s.r. work; this latter does not reveal evidence for large rhombic distortions as implied by Pope's arguments. A consequence of the lowering of symmetry is that the molecular orbital scheme of Ballhausen and Gray [82] (Fig. 8) is only applicable to $[Mo_6O_{19}]^{3-}$ and not strictly to other, i.e. 12- and 18-, molybdates. However the lowering of the symmetry causes the E state to be split into two components labelled γ_1 and γ_2 (see diagram below). Furthermore the larger Mo–O–Mo angles in 12- and 18-molybdates, as opposed to those in $[Mo_6O_{19}]^{3-}$, imply an enhanced equatorial Mo–O π-bonding. Thus the non-bonding B_2 state becomes weakly anti-bonding.

The description, although in Pope's words a "crude" one, of the IVCT transitions then involves electronic transitions between metal sites (1) and (2). For 12- and 18-molybdates the band in the electronic spectrum at 8000–10000 cm^{-1} can be assigned to $B_2(2) \leftarrow B_2(1)$ and that at 13000–16000 cm^{-1} to $\gamma_1(2) \leftarrow B_2(1)$. The 18000–20000 cm^{-1} band assigned to $^2B_1 \leftarrow {}^2B_2$

for Mo^{V} by Fruchart et al. [69] is more likely to arise from the $\sigma^* \leftarrow \pi$, Mo ← O charge transfer, as proposed by Garner et al. [104].

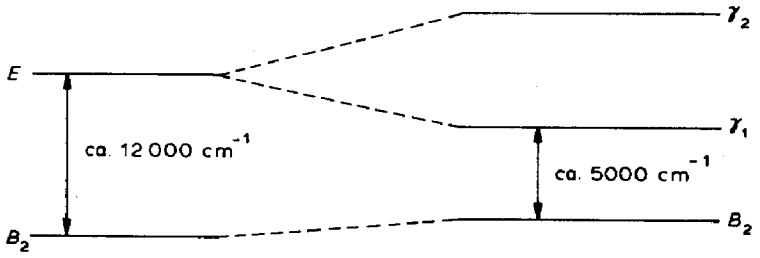

Mo_6O_{19}
C_{4v}
little equatorial
π-bonding

$XMo_{12}O_{40}$, $X_2Mo_{18}O_{62}$
rhombic (C_s)
enhanced equatorial
π-bonding

REFERENCES

1 (a) R.J.H. Clark and D. Brown, The Chemistry of Vanadium, Niobium and Tantalum, Pergamon Press, Oxford, 1973.
(b) C.L. Rollinson, The Chemistry of Chromium, Molybdenum and Tungsten, Pergamon Press, Oxford, 1973.
(c) M.T. Pope, Heteropoly and Isopoly Oxometalates, Springer-Verlag, Berlin, 1983.
2 J.D.H. Strickland, J. Am. Chem. Soc., 74 (1952) 862.
3 T.J.R. Weakley, Struct. Bond. (Berlin), 18 (1974) 131.
4 M.T. Pope, Heteropoly Blues, in D.B. Brown (Ed.), Mixed-Valence Compounds, Proc. NATO Adv. Study Inst., Oxford, 1979.
5 (a) M.B. Robin and P. Day, Adv. Inorg. Chem. Radiochem., 10 (1967) 247.
(b) R.J.H. Clark, Chem. Soc. Rev., 13 (1984) 219.
6 K.H. Tytko and O. Glemser, Adv. Inorg. Chem. Radiochem., 24 (1981) 239.
7 M.T. Pope, Inorg. Chem., 8 (1972) 1973.
8 K. Nomiya and M. Makoto, Polyhedron, 3 (1984) 341.
9 P. Souchay and J. Faucherre, Bull. Soc. Chim. Fr., 18 (1951) 355.
10 M. Biquard and M. Lamache, Bull. Soc. Chim. Fr., (1971) 32.
11 T. Yamase, J. Chem. Soc., Dalton Trans., (1982) 1987.
12 T. Yamase and K. Tadatoshi, J. Chem. Soc., Dalton Trans., (1983) 2205.
13 I. Pascaru, O. Constantinescu, M. Constantinescu, and D. Arizan, J. Chim. Phys., 62 (1965) 1283.
14 (a) J.F. Keggin, Nature, 131 (1933) 908.
(b) J.F. Keggin, Proc. R. Soc. London, Ser. A, 144 (1934) 75.
15 (a) I. Lindqvist, Ark. Kemi, 5 (1953) 217.
(b) I. Lindqvist and B. Aaronsson, Ark. Kemi, 7 (1955) 49.
16 B. Dawson, Acta Crystallogr., 6 (1953) 113.
17 M.T. Pope, Inorg. Chem., 15 (1976) 2008.
18 L.C.W. Baker and J.S. Figgis, J. Am. Chem. Soc., 92 (1970) 3794.
19 R. Thouvenot, M. Fournier, R. Franck, and C. Rocchiccioli-Deltcheff, Inorg. Chem., 23 (1984) 598.

19 (a) J.N. Barrows, G.B. Jameson and M.T. Pope, J. Am. Chem. Soc., in press.
20 H.T. Evans, Perspect. Struct. Chem., 4 (1971) 1.
21 C. Rocchiccioli-Deltcheff, M. Fournier, R. Franck, and R. Thouvenot, Inorg. Chem., 22 (1983) 207.
22 C. Sanchez, J. Livage, J.P. Launay, M. Fournier, and Y. Jeannin, J. Am. Chem. Soc., 104 (1982) 3194.
23 D.L. Kepert, The Early Transition Metals, Academic Press, London, 1972.
24 C. Rocchiccioli-Deltcheff and R. Thouvenot, J. Chem. Res., (S) (1977) 46; (M) (1977) 0549.
25 E.N. Yurchenko, J. Mol. Struct., 60 (1980) 325.
25 (a) H.T. Evans and M.T. Pope, Inorg. Chem., 23 (1984) 501.
26 R. Strandberg, Acta Chem. Scand., Ser. A, 29 (1975) 350.
27 (a) P. Souchay, R. Contant, and J.M. Fruchart, C.R. Acad. Sci., Ser. C, 246 (1967) 976.
(b) J.M. Fruchart and P. Souchay, C.R. Acad. Sci., Ser. C, 266 (1968) 1571.
(c) R. Contant, C.R. Acad. Sci., Ser. C, 267 (1968) 1479.
28 C. Rocchiccioli-Deltcheff, M. Fournier, R. Franck, and R. Thouvenot, J. Mol. Struct., 114 (1984) 49.
29 (a) H.R. Allcock, E.C. Bissell, and E.T. Shawe, Inorg. Chem., 12 (1973) 2963.
(b) C.D. Garner, N.C. Howlader, F.E. Mabbs, A.T. McPhail, R.W. Miller, and K.D. Onan, J. Chem. Soc., Dalton Trans., (1978) 1582.
(c) O. Nagaro and Y. Sasaki, Acta Crystallogr., Sect. B, 35 (1979) 2387.
30 R. von Mattes, H. Bierbüsse, and J. Fuchs, Z. Anorg. Allgem. Chem., 385 (1971) 230.
31 C. Rocchiccioli-Deltcheff, R. Thouvenot, and M. Fouassier, Inorg. Chem., 21 (1982) 30.
32 F.J. Farrell, V.A. Maroni, and T.G. Spiro, Inorg. Chem., 8 (1969) 2638.
33 E.B. Wilson, J.C. Decius, and P.C. Cross, Molecular Vibrations, McGraw-Hill, New York, 1955.
34 R.I. Buckley and R.J.H. Clark, to be published.
35 S.B. Piepho, E.R. Krausz, and P.N. Schatz, J. Am. Chem. Soc., 100 (1978) 2996.
36 K.Y. Wong and P.N. Schatz, Prog. Inorg. Chem., 28 (1981) 369.
37 N.E. Sharpless and J.S. Munday, Anal. Chem., 29 (1957) 1619.
38 P. Rabette and D. Olivier, Rev. Chem. Mineral., 7 (1970) 181.
39 G. Lange, H. Hahn, and K. Dehnicke, Z. Naturforsch., Teil B, 24 (1969) 1498.
40 J. Fuchs, Z. Naturforsch., Teil B, 28 (1973) 389.
41 C. Rocchiccioli-Deltcheff, R. Thouvenot, and R. Franck, Spectrochim. Acta, Part A, 32 (1976) 143, 587.
42 R. Thouvenot, C. Rocchiccioli-Deltcheff, and P. Souchay, C.R. Acad. Sci., Ser. C, 278 (1974) 455.
43 C. Rocchiccioli-Deltcheff and R. Thouvenot, Colloq. Spectrosc. Int. (Proc.), 18th, 2 (1975) 500.
44 L. Lyhamn, S.J. Cyvin, B.N. Cyvin, and J. Brunvoll, Spectrosc. Lett., 9 (1976) 859.
45 L. Lyhamn, S.J. Cyvin, B.N. Cyvin, and J. Brunvoll, Z. Naturforsch., Teil A, 31 (1976) 1589.
46 L. Lyhamn and S.J. Cyvin, Spectrosc. Lett., 10 (1977) 907.
47 L. Lyhamn, S.J. Cyvin, B.N. Cyvin, and J. Brunvoll, Spectrosc. Lett., 12 (1979) 101.
48 S.J. Cyvin, L. Lyhamn, and B.N. Cyvin, Monatsh. Chem., 110 (1979) 311.
49 M.S. Kasprzak, G.E. Leroi, and S.R. Crouch, Appl. Spectrosc., 36 (1982) 285.
50 R. Andreassen, S.J. Cyvin, and L. Lyhamn, J. Mol. Struct., 25 (1975) 155.
51 N.S. Tasasova, L.P. Kazanskii, and E.N. Dorokhova, Russ. J. Inorg. Chem., 26 (1981) 338.
52 M. Akimoto and E. Echigoya, Chem. Lett., (1981) 1759.

53 T. Tsai, K. Maruya, M. Ai, and A. Ozaki, Bull. Chem. Soc. Jpn., 55 (1982) 949.
54 H. Tsuneki, H. Niyama, and E. Echigoya, Chem. Lett., (1978) 645, 1183.
55 N. Mizuno, K. Katamura, Y. Yoneda, and M. Misono, J. Catal., 83 (1983) 384.
56 R.I. Buckley and R.J.H. Clark, unpublished work.
57 M.T. Pope, S.E. O'Donnell, and R.A. Prados, J. Chem. Soc., Chem. Commun., (1975) 22.
58 J.J. Altenau, M.T. Pope, R.A. Prados, and H. So, Inorg. Chem., 14 (1975) 417.
59 E.N. Yurchenko and V.I. Bugaev, J. Mol. Struct., 115 (1984) 71.
60 R.J.H. Clark and B. Stewart, Struct. Bonding (Berlin), 36 (1979) 1.
61 G.A. Tsigdinos and C.J. Hallada, Inorg. Chem., 7 (1968) 437.
62 C.D. Ai, H.G. Jerschkewitz, P. Reich, and E. Schreier, Z. Chem., 22 (1982) 419.
63 L. Lyhamn, Chem. Scr., 12 (1977) 153.
64 L. Lyhamn and L. Pettersson, Chem. Scr., 12 (1977) 142.
65 N.S. Hush, Progr. Inorg. Chem., 8 (1967) 391.
66 K.B. Yatsimirskii and I.I. Alekseeva, Russ. J. Inorg. Chem., 8 (1963) 1317.
67 H. So and M.T. Pope, Inorg. Chem., 11 (1972) 1441.
68 P.J. Coope and W.P. Thistlethwaite, J. Inorg. Nucl. Chem., 2 (1956) 125. (See also F. Chauveau, R. Schaal, and P. Souchay, C.R. Acad. Sci., 240 (1955) 194.
69 J.M. Fruchart, G. Herve, J.P. Launay, and R. Massart, J. Inorg. Nucl. Chem., 38 (1976) 1627.
70 M. Ché, M. Fournier, and J.P. Launay, J. Chem. Phys., 71 (1979) 1954.
71 Y. Jeannin, J.P. Launay, C. Sanchez, J. Livage, and M. Fournier, Nouv. J. Chim., 4 (1980) 587.
72 F. Chauveau, Bull. Soc. Chim. Fr., (1960) 834.
73 D. Labonnette and S. Ostrowetsky, C.R. Acad. Sci., Ser. C, 282 (1976) 341.
74 D. Labonnette, J. Chem. Res., (S) 252; (M) 2801 (1979).
75 G. Herve and A. Teze, Inorg. Chem., 16 (1977) 2115.
76 F. Robert and A. Teze, Acta Crystallogr., Sect. B, 37 (1981) 318.
77 R. Massart, Ann. Chim., 4 (1969) 367.
78 N. Tanaka, K. Unowa, and E. Itabashi, Inorg. Chem., 21 (1982) 1662.
79 G.H. Back and H. So, J. Korean Chem. Soc., 19 (1975) 207.
80 E. Papaconstantinou and M.T. Pope, Inorg. Chem., 9 (1970) 667.
81 E. Papaconstantinou and M.Z. Hoffman, Inorg. Chem., 21 (1982) 2087.
82 C.J. Ballhausen and H.B. Gray, Inorg. Chem., 1 (1962) 111.
83 J.P. Launay, M. Fournier, C. Sanchez, J. Livage, and M.T. Pope, Inorg. Nucl. Chem. Lett., 16 (1980) 257.
84 P. Rabette, C. Ropars, and J.P. Grivet, C.R. Acad. Sci., Ser. C, 265 (1967) 153.
85 (a) M.T. Pope, S.E. O'Donnell, and R.A. Prados, Proc. Conf. Coord. Chem., 16th (Dublin, 1974) 3.10.
(b) R.A. Prados, P.T. Meiklejohn, and M.T. Pope, J. Am. Chem. Soc., 96 (1974) 1261.
86 R.A. Prados and M.T. Pope, Inorg. Chem., 15 (1976) 2547.
87 M.M. Zaitov, Russ. J. Inorg. Chem., 20 (1975) 1726.
88 K. Eguchi, N. Yamazoe, and T. Seiyama, Chem. Lett., (1982) 1341.
89 M. Otake and T. Otaki, Bull. Chem. Soc. Jpn., 48 (1975) 55.
90 M. Otake, Y. Komiyama, and T. Otaki, J. Phys. Chem., 77 (1973) 2896.
91 R.I. Maksimovskaya, M.A. Fedotov, L.I. Kuznetsova, V.M. Mastikhin, and K.I. Matveev, Dokl. Phys. Chem., 223 (1975) 725.
92 R.J.H. Clark and T.J. Dines, Mol. Phys., 42 (1981) 193.
93 T. Yamase, T. Ikawa, H. Kokado, and E. Inoue, Chem. Lett., (1973) 615.
94 T. Yamase, H. Hayashi, and T. Ikawa, Chem. Lett., (1974) 1055.

95 T. Yamase and T. Ikawa, Bull. Chem. Soc. Jpn., 50 (1977) 746.
96 T. Yamase, J. Chem. Soc., Dalton Trans., (1978) 283.
97 T. Yamase, R. Sasaki, and T. Ikawa, J. Chem. Soc., Dalton Trans., (1981) 628.
98 T. Yamase and T. Kurozumi, Inorg. Chim. Acta, 83 (1984) L25.
99 T. Yamase, Inorg. Chim. Acta, 64 (1982) L155.
100 (a) T. Yamase and T. Ikawa, Inorg. Chim. Acta, 37 (1979) L529.
(b) T. Yamase and T. Ikawa, Inorg. Chim. Acta, 45 (1980) L55.
101 T. Yamase, Inorg. Chim. Acta, 54 (1981) L207.
102 C.R. Byfleet, F.G. Herring, W.C. Lin, C.A. McDowell, and D.J. Ward, Mol. Phys., 15 (1968) 239.
103 M.T. Pope, Heteropoly and Isopoly Oxometalates, Springer-Verlag, Berlin, 1983.
104 C.D. Garner, L. Hill, N.C. Howlader, M.R. Hyde, F.E. Mabbs, and V.I. Routledge, Proc. 2nd Int. Conf. Chemistry and Uses of Molybdenum, Climax Molybdenum Co., Oxford, 1976, p. 13.